VULNERABILITY, IMPACTS AND ADAPTATION ASSESSMENT IN THE EAST AFRICA REGION

CHAPTER 7: CLIMATE CHANGE SCENARIOS: PROJECTED RAINFALL AND TEMPERATURE

NOVEMBER 2017

This report was produced for review by the United States Agency for International Development. It was prepared by Camco Advisory Services (K) Ltd. under subcontract to Tetra Tech ARD.

This report was produced for review by Camco Advisory Services (K) Ltd. under subcontract to Tetra Tech ARD, through USAID/Kenya and East Africa Contract No. AID-623-C-13-00003.

CONTRIBUTORS:
Hussen Endris[1], Herbert Misiani[1], Geoffrey Sabiiti[1], Mohammed Y Said[2], Joseph O Ogutu[3], Christopher Oludhe[4], Philip Omondi[5], Gideon Galu[6], Gilbert Ouma[4] and Matayo Indeje[7]

[1]IGAD Climate Prediction and Applications Centre (*ICPAC),* P.O. BOX 10304, 00100 - Dagoretti Corner, Nairobi, Kenya

[2]Centre for Sustainable Dryland Ecosystems and Societies (*CSDES),* University of Nairobi, P.O. Box 30197-00100 Nairobi, Kenya

[3]University of Hohenheim, Schloss Hohenheim 1, 70599 Stuttgart, Germany

[4]University of Nairobi, Institute for Climate Change and Adaptation. P.O Box 30197-00100 Nairobi, Kenya

[5]World Food Programme, UN Gigiri Compound, Nairobi, Kenya

[6]USGS/FEWS NET, P.O. Box 66613, Nairobi, Kenya

[7]Planning for Resilience in East Africa through Policy, Adaptation, Research and Economic Development (PREPARED), Nairobi, Kenya

Tetra Tech ARD
159 Bank Street, Suite 300
Burlington, Vermont 05401 USA

Tetra Tech ARD Contacts:

Anna Farmer
Project Manager
Tetra Tech
Burlington, Vermont
Tel.: (802) 658-3890
Anna.Farmer@tetratech.com

Korinne Nevins
Assistant Project Manager
Tetra Tech
Burlington, Vermont
Tel.: (802) 658-3890
Korinne.Nevins@tetratech.com

VULNERABILITY, IMPACTS AND ADAPTATION ASSESSMENT IN THE EAST AFRICA REGION

CHAPTER 7:

CLIMATE CHANGE SCENARIOS: PROJECTED RAINFALL AND TEMPERATURE

NOVEMBER 2017

DISCLAIMER
This report is made possible by the generous support of the American people through the United States Agency for International Development (USAID). The views expressed are those of the authors and do not necessarily reflect the views of USAID or the United States Government.

ACRONYMS

CORDEX	Coordinated Regional Climate Downscaling Experiment
EAC	East African Community
GCM	Global climate models
IOD	Indian Ocean Dipole
LVB	Lake Victoria Basin
PREPARED	Planning for Resilience in East Africa through Policy, Adaptation, Research, and Economic Development
RCA	Rossby Centre Regional Atmospheric model
USAID	United States Agency for International Development
VIA	Vulnerability, Impact, and Adaptation Assessment
DJF	December-January-February
ENSO	El Niño Southern Oscillation
IPCC	Intergovernmental Panel on Climate Change
MAM	March-April-May
MPI	Max Planck Institute
OND	October-November-December
SRES	Special Report on Emissions Scenarios
VIA	Vulnerability, Impacts and Adaptation Assessment

CONTENTS

ACRONYMS 2
CONTENTS 3
BACKGROUND 4
CLIMATE CHANGE SCENARIOS AND PROJECTED RAINFALL AND TEMPERATURE FOR EAST AFRICA 6
Downscaling of the Climate Models and Assumptions *6*
Description of the Three Climate Scenarios *6*
Projected Changes in Rainfall and Temperature over Eastern Africa *8*
Rainfall *8*
Maximum Temperature *10*
Minimum Temperature *13*
MAPPING OF EXTREME EVENTS—CHANGES IN THE PROJECTED RAINFALL AND TEMPERATURE EXTREMES 16
Data and Methods *16*
Difference in the 5th Percentile of Rainfall *16*
Difference in the 95th Percentile of Rainfall *19*
Difference in the 10th Percentile of the Maximum Temperature *22*
Difference in the 90th Percentile of Maximum Temperature *24*
Difference in the 10th Percentile of the Minimum Temperature *27*
Difference in the 90th Percentile of the Minimum Temperature *29*
HIGHLIGHTS 31
Modeling *31*
RESULTS 32
Rainfall *32*
Maximum Temperature *32*
Minimum Temperature *32*
REFERENCES 34

BACKGROUND

Sub-Saharan Africa is a rapidly developing region of more than 973 million people (in 2014), with 49 countries, and great ecological, climatic, and cultural diversity. The population for 2050 is projected to approach 1.5 to 2 billion people (United Nations, Department of Economic and Social Affairs, Population Division 2015).

The region is confronted with a range of climate risks that could have far-reaching repercussions for its communities and economies in future. Even if warming is limited below 2°C, there are very substantial risks and projected damages, and as warming increases these are only expected to grow further (World Bank 2013). The Fourth and Fifth Assessment Reports (AR4 and AR5) of the IPCC (2007, 2013) and the World Bank (2013) summarize the projected impacts of climate change on the African region. Likely physical and biophysical impacts as a function of projected climate change are as follows:

Water availability: Under 2°C warming the existing differences in water availability across the region could become more pronounced. IPCC (2007) predicts that 90 million to 220 million people in Africa would be exposed to increased water stress due to climate change. This magnifies water woes in a region already dealing with water-related problems.

Projected aridity trends: Aridity is projected to spread due to changes in temperature and precipitation, most notably in southern Africa. In a 4°C world, total hyper-arid and arid areas are projected to expand by 10 percent compared to the 1986–2005 period. Where aridity increases, crop yields are likely to decline as the growing season shortens.

Regime shifts in African ecosystems: The projected shifts could result in a reduction in the extent of savanna grasslands. By the time 3°C global warming is reached, savannas are projected to decrease to approximately one-seventh of total current land area, reducing the availability of forage for grazing animals. Projections indicate that species composition of local ecosystems might shift, and negatively affect the livelihood strategies of communities dependent on them.

Agricultural production: Production is likely to be affected in the near-term, as warming shifts the climatic conditions that are conducive to current agricultural production. The area of land suitable for agriculture, length of growing seasons, and yield potential are expected to shrink—particularly along the margins of semi-arid and arid areas. Food security would be adversely affected, and malnutrition exacerbated. The annual average temperature is already above optimal values for wheat during the growing season over much of Sub-Saharan Africa and non-linear reductions in maize yield above certain temperature thresholds have been reported. Significant impacts are expected well before mid-century even for relatively low levels of warming. For example, a 1.5°C warming by the 2030s could lead to about 40 percent of present maize cropping areas being no longer suitable for current cultivars. Under warming of less than 2°C by the 2050s, total crop production could be reduced by 10 percent. For higher levels of warming there are indications that yields may decrease by around 15–20 percent across all crops and regions. Heat and drought would also result in severe losses of livestock and associated impacts on rural communities.

Human health: Several health issues expected to worsen with climate change—undernourishment, childhood stunting, malaria, and other diseases—could undermine childhood educational performance. Rates of undernourishment are already high, ranging between 15 and 65 percent, depending on sub-region. With warming of 1.2–1.9°C by 2050, the undernourished population is projected to increase by 25–90 percent compared to the present. Other impacts

expected to accompany climate change include mortality and morbidity due to extreme events such as high temperatures, drought, and flooding. IPCC (2007) report predicts a 5–7 percent potential increase in malaria distribution by the end of the century. Previously malaria-free highland areas in Burundi, Ethiopia, Kenya, and Rwanda could also experience malaria starting from around mid-century, potentially exposing communities with little or no immunity to a debilitating illness.

These global and continental studies have prompted more regional- or country-focused studies on the impacts of climate to change to various sectors. The Planning for Resilience in East Africa through Policy, Adaptation, Research, and Economic Development (PREPARED) program for the Lake Victoria Basin (PREPARED 2013, 2014) is a medium-term (five-year), multi-organization, comprehensive program aimed at mainstreaming integrated, multisectoral, evidence-based, climate-resilient development planning and program implementation into the development agendas of the East African Community (EAC) and its Partner States. PREPARED consists of five components: the first three address climate change adaptation, biodiversity conservation, and water supply, sanitation and hygiene. The other two pertain to program coordination of crosscutting elements and project management. As part of the climate change adaptation, PREPARED aims to assist EAC Partner States to undertake Vulnerability, Impacts and Adaptation Assessment (VIA). The climate-sensitive sectors under this assessment include: Water, Aquatic Ecosystems, and Water Supply Infrastructure; Terrestrial Ecosystems, including Forestry, Wildlife, and Tourism; Agriculture and Food Security; Health, Sanitation, and Human Settlements; and Energy and Transport Infrastructure.

This study aims to identify key climate change risks and vulnerabilities within the Lake Victoria Basin (LVB) and facilitates the development of a LVBC Climate Change Adaptation Strategy and Action Plan. This chapter introduces the historical and projected future climate in East Africa as a basis for the rest of the VIA.

CLIMATE CHANGE SCENARIOS AND PROJECTED RAINFALL AND TEMPERATURE FOR EAST AFRICA

DOWNSCALING OF THE CLIMATE MODELS AND ASSUMPTIONS

Global climate models (GCMs), forced with scenarios for the evolution of concentrations of greenhouse gases and aerosols, are the fundamental tools for projecting climate change into the future. However, because of their complexity and the need to perform iterative simulations, GCM simulations are very demanding in computational resources and are performed at relatively coarse horizontal resolution. Hence, they are not necessarily capable of capturing the detailed processes associated with regional-local climate variability and changes that are required for accurate regional and national climate change assessments. Not surprisingly, then, GCMs only provide information at spatial scales coarser than those typically required for developing reliable local-level adaptation and mitigation strategies.

The limitations of GCMs can be overcome by using regional climate models (RCMs) to dynamically downscale the coarse-resolution GCM outputs to scales more suited to regional, national, and local end-users over geographic regions of interest. RCMs use the information derived from GCM simulations to define the surface and lateral boundary conditions. This enables RCMs to better represent topographical details, coastlines, and land-surface heterogeneities, and hence to more faithfully reproduce small-scale processes and details that are essential to developing reliable climate change impact assessment for regional, national, and local adaptation policies and interventions.

Recently, the Coordinated Regional Climate Downscaling Experiment (CORDEX) program, initiated by the World Climate Research Program, provided the opportunity for generating high-resolution regional climate projections for use in assessing the future impacts of climate change at regional scales (Giorgi et al. 2009).

In this report, we used simulated data from the Rossby Center regional atmospheric model (RCA4) driven by the Earth system version of the Max Planck Institute for Meteorology (MPI-ESM-LR) coupled global climate model from the ongoing CORDEX project. The model was integrated into the CORDEX-Africa domain (see Nikulin et al. 2012, Endris et al. 2013), with a horizontal grid spacing of 0.44 degrees. The historical simulations were forced by observed natural and anthropogenic atmospheric composition covering the period 1950–2005, and the projections for 2006–2100 were forced by Representative Concentration Pathways (RCPs). The choice of the RCA model–driven MPI-ESM-LR for this analysis was based primarily on the availability of the model outputs for the three different scenarios (RCP2.6, RCP4.5, and RCP8.5), as the other model runs were available for only one or two of the three scenarios. Moreover, a recent assessment study (Endris et al. 2015) has shown that the RCA model driven by MPI-ESM-LR better reproduces large-scale signals such as the El Niño Southern Oscillation (ENSO) and the Indian Ocean Dipole (IOD) in the historical period over the East Africa region than RCA model run driven by the other GCMs.

DESCRIPTION OF THE THREE CLIMATE SCENARIOS

The simulations used for the projections are forced by the RCPs, which are based on radiative forcings (globally radiative energy imbalance) measured in Wm^{-2} by the year 2100 (Moss et al. 2010). Three RCPs are used—RCP2.6, RCP4.5, and RCP8.5—which represent the low, mid, and high-level emission and concentration scenarios, respectively. The RCP2.6 emission and

concentration pathway, also referred to as RCP3PD (Peak and Decline), represents a peak in radiative forcing at ~3 W/m² (~490 ppm CO_2) by the mid-twenty-first century and then a decline to 2.6 W/m² by 2100. This scenario assumes optimistic mitigation measures and that the increase in the global average temperature will be limited below 2°C. RCP4.5 is a medium concentration pathway that is assumed to stabilize radiative forcing at 4.5 W/m² (~650 ppm CO_2) and that this value will not be exceeded by the year 2100. The RCP8.5 pathway is a high-concentration pathway in which radiative forcing is assumed to reach 8.5 W/m² by the year 2100 (~1370 ppm CO_2) and then continues to rise thereafter. The RCP8.5 socioeconomic pathway is characterized by rapidly rising population and relatively slow income growth with modest rates of technological change and energy intensity improvements, leading to high energy demands and greenhouse gas emissions in the absence of climate change policies (Riahi et al. 2011).

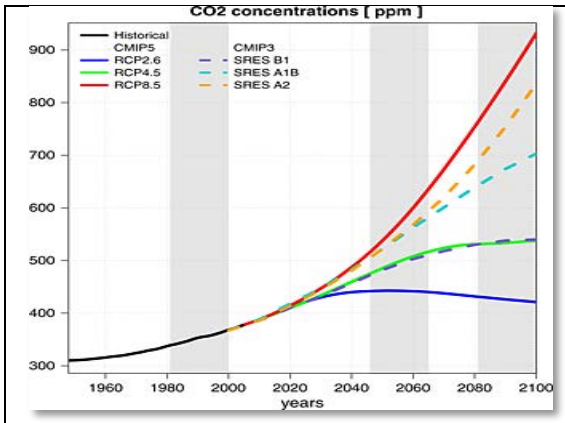

Figure 1: Concentration of carbon dioxide (CO_2) across the three RCPs. The dotted lines indicate three of the SRES marker scenarios.[1] Source: Van Vuuren et al. 2011.

The analysis used in this report utilized downscaled rainfall, maximum and minimum temperature model outputs from the Rossby Centre Regional Atmospheric (RCA) mode driven by one of the CMIP5 (Max Planck Institute; MPI) global circulation models as boundary conditions. The data are at a resolution of 50 kilometers by 50 kilometers and cover the Africa domain. Downscaled data are available for historical (1951–2005) and projection (2006–2100) periods for the RCP2.6, RCP4.5, and RCP8.5 scenarios.

[1] The IPCC published a new set of scenarios in 2000 for use in the Third Assessment Report (Special Report on Emissions Scenarios - SRES). The SRES scenarios were constructed to explore future developments in the global environment with special reference to the production of greenhouse gases and aerosol precursor emissions. The SRES team defined four narrative storylines labelled A1, A2, B1, and B2, describing the relationships between the forces driving greenhouse gas and aerosol emissions and their evolution during the twenty-first century for large world regions and globally. Each storyline represents different demographic, social, economic, technological, and environmental developments that diverge in increasingly irreversible ways. Representative Concentration Pathways (*RCPs*) are four greenhouse gas concentration (not emissions) trajectories adopted by the IPCC for its Fifth Assessment Report (AR5) in 2014. It supersedes SRES projections published in 2000.

PROJECTED CHANGES IN RAINFALL AND TEMPERATURE OVER EASTERN AFRICA

The projected changes in rainfall, and maximum and minimum temperatures based on the RCP2.6, RCP4.5, and RCP8.5 scenarios have been analyzed for four future time slices: 2020s (2006–2035), 2030s (2016–2045), 2050s (2036–2065), and 2070s (2055–2085) to provide information on the expected magnitude of the climate response over each time window. The period 1971–2000 is considered as a reference for the present climate. The projected climates change signals for each time window are calculated as the difference between the future time windows (averages calculated over 30 years) and the reference period. For example, the rainfall change by 2070s is computed based on the difference in average rainfall between 2055–2085 and the reference period 1971–2000 (ICPAC 2016, Giorgi 2006).

RAINFALL

Figures 2 to 3 show the projected changes in the annual and seasonal rainfall components over the EAC region for the 2020s, 2030s, 2050s, and 2070s under the three scenarios, relative to the reference period (1971–2000). The projected changes in the annual rainfall component under each of the three scenarios and time windows show relatively little change compared to the projected changes in the seasonal rainfall components. The short rains (October–December or OND period) are projected to increase over most parts of the region under all the three scenarios (5–25 percent by 2020 and 2030, and 25–50 percent by 2050 and 2070). By contrast, the long rains (March–May or MAM period) are projected to decrease over the northern part but to increase over the south eastern part of the region. The June–September dry (JJAS) season, when the western and coastal parts of the region receive substantial amount of rainfall, is projected to decrease over most parts of the region (25–50 percent by 2020 and 2030, and 50–75 percent by 2050 and 2070). The projected annual rainfall generally shows a tendency to increase over the LVB except for JJAS in 2020 for RCP8.5 and 2070 for RCP2.6.

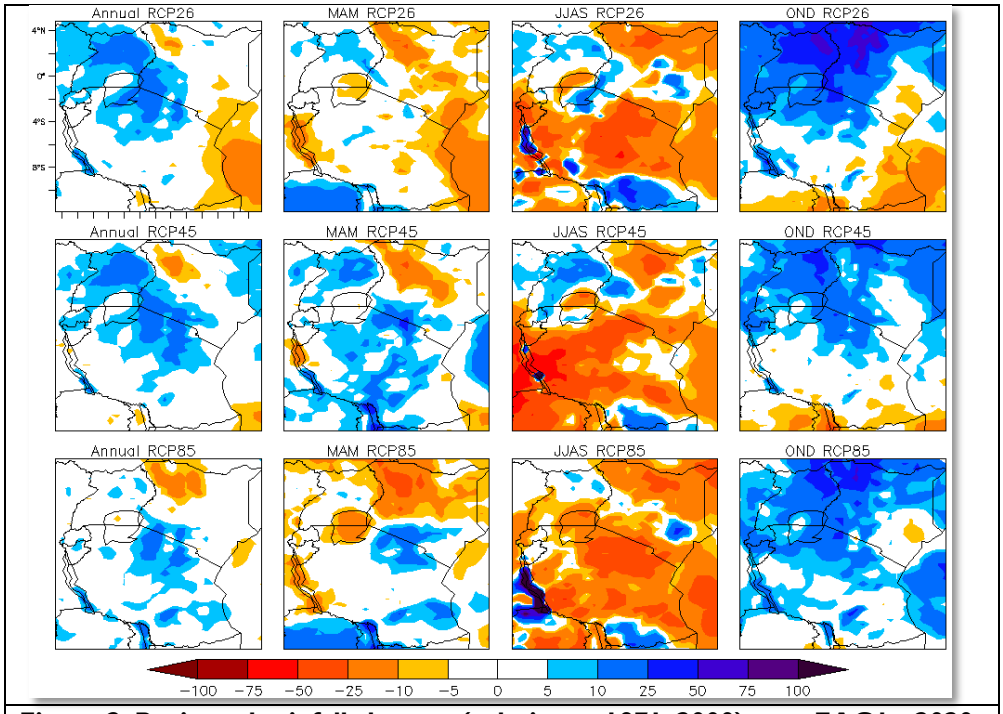

Figure 2: Projected rainfall changes (relative to 1971–2000) over EAC by 2020s in annual (1st column), MAM (2nd column), JJAS (3rd column), OND (4th

column). Each row corresponds to emission scenarios: RCP2.6 (1st row), RCP4.5 (2nd row), and RCP8.5 (3rd row).

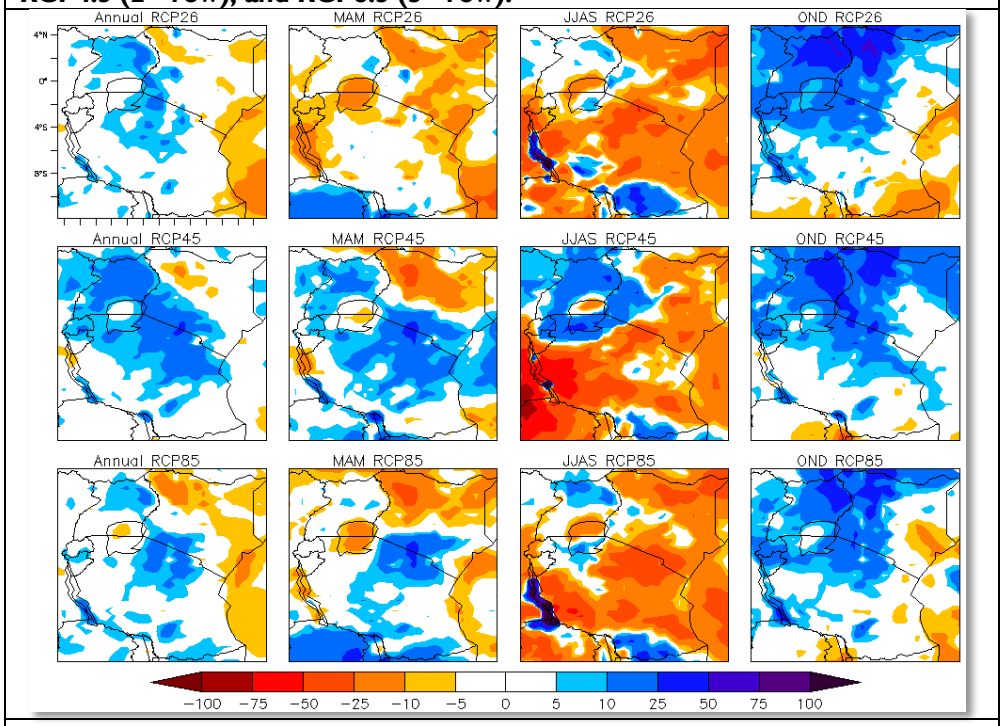

Figure 3: Projected rainfall changes over EAC by 2030s in annual (1st column), MAM (2nd column), JJAS (3rd column), OND (4th column). Each row corresponds to emission scenarios: RCP2.6 (1st row), RCP4.5 (2nd row), and RCP8.5 (3rd row).

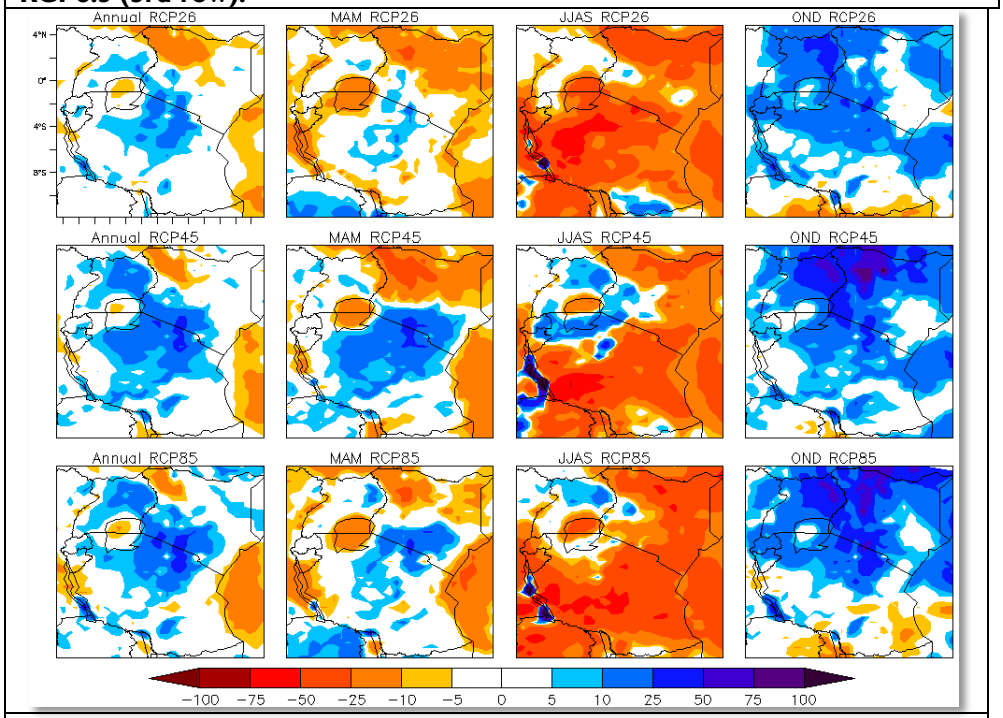

Figure 4: Projected rainfall changes over EAC by 2050s in annual (1st column), MAM (2nd column), JJAS (3rd column), OND (4th column). Each row corresponds to emission scenarios: RCP2.6 (1st row), RCP4.5 (2nd row), and

RCP8.5 (3rd row).

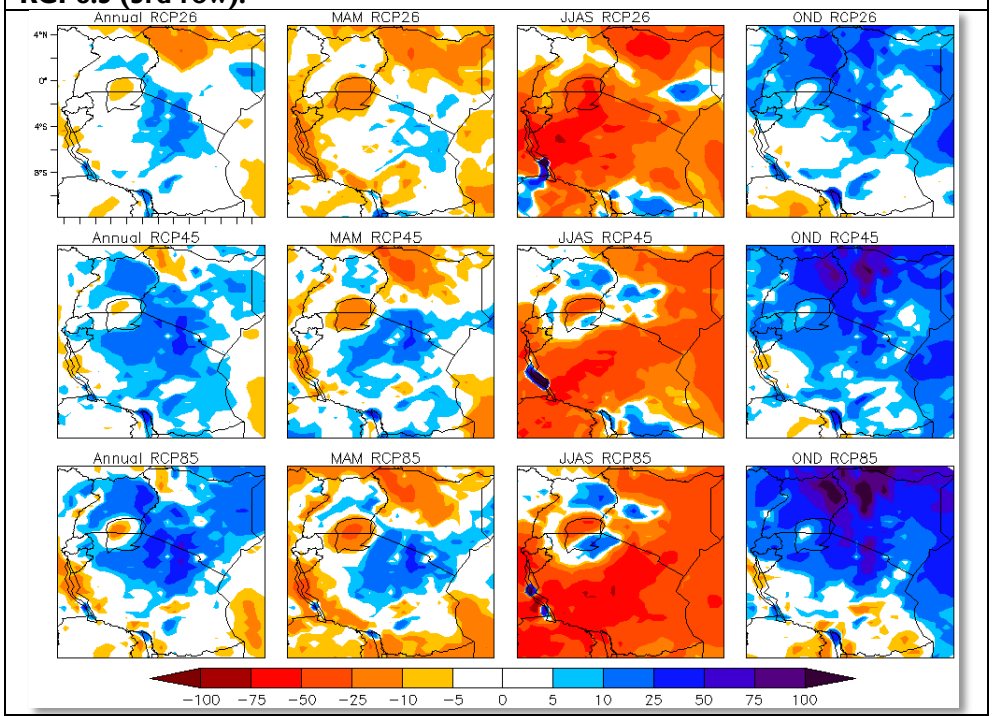

Figure 5: Projected rainfall changes over EAC by 2070s in annual (1st column), MAM (2nd column), JJAS (3rd column), OND (4th column). Each row corresponds to emission scenarios: RCP2.6 (1st row), RCP4.5 (2nd row), and RCP8.5 (3rd row).

MAXIMUM TEMPERATURE

The projected changes in the maximum temperature component for the three scenarios (RCP2.6, RCP4.5, and RCP8.5) in the 2020s, 2030s, 2050s, and 2070s periods compared to the reference period (1971–2000) are shown in Figures 2a–d. The projected temperature changes for the three different scenarios and time windows show relatively large changes compared to the projected changes in the seasonal components. By 2020, annual maximum temperatures are anticipated to be 0.5 to 1.0°C higher under the RCP2.6 and RCP4.5 scenarios but 0.5 to 1.5°C higher under the RCP8.5 scenario over most parts of the EAC, with slightly less warming apparent in some coastal areas. By 2030, maximum temperatures during the long rains (MAM), the dry season (JJAS), and throughout the year (annual component) will likely increase by 1.0 to 2.0°C over most parts of the region, but with spatial variation like that of 2020. The expected warming extent is greatest during the long rains (MAM) and the dry season (JJAS) and least during the short rains (OND).

By 2050, annual maximum temperatures are expected to be 1.0 to 2.0°C higher under the RCP2.6, 1.5 to 2.5°C higher under the RCP4.5 and 2.5 to 3.5°C higher under the RCP8.5 scenarios over most parts of the EAC, with slightly less warming expected in some coastal areas. The greatest potential warming will likely occur in the dry season (JJAS) and during the long rains (MAM). In the far future (2070), projected annual maximum temperatures will likely be 0.5 to 1.5°C higher under the RCP 2.6 scenario, which is notably smaller than the changes anticipated by 2050. This is due to the reduction in radiative forcing expected toward the end of the century due to mitigation measures under the RCP 2.6 scenario. In contrast, under the RCP8.5 scenario, the

expected annual warming will likely result in temperatures 3.5 to 4.5°C higher than the reference period, with far greater warming expected during the dry season (JJAS).

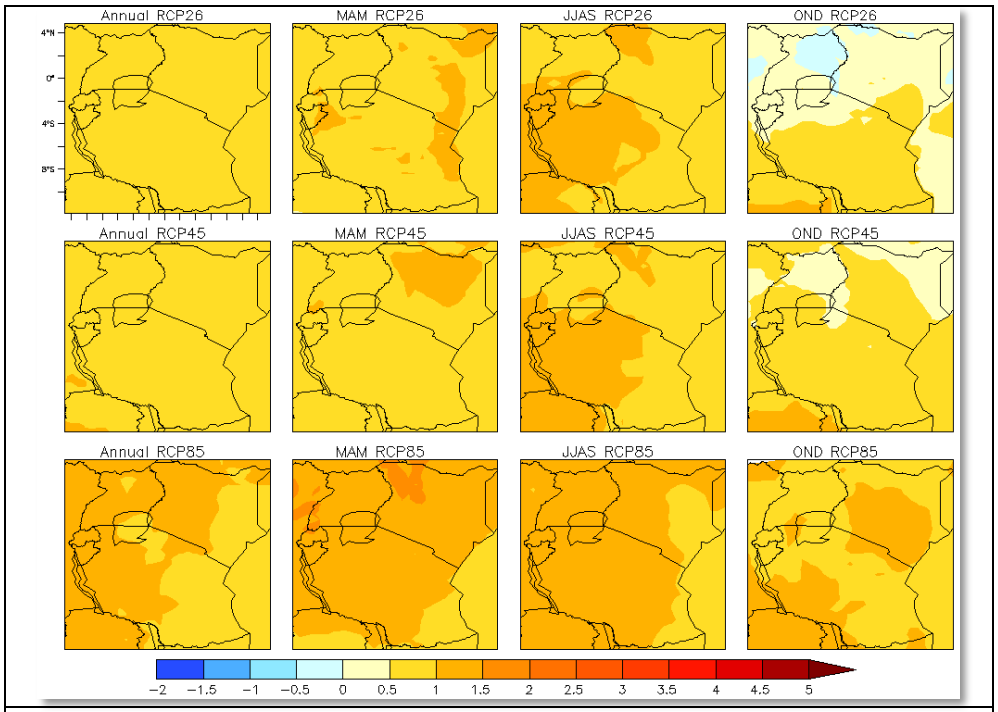

Figure 6: Projected maximum temperature changes over the EAC by the 2020s in annual (1st column), MAM (2nd column), JJAS (3rd column), OND (4th column). Each row corresponds to emission scenarios: RCP2.6 (1st row), RCP4.5 (2nd row), and RCP8.5 (3rd row).

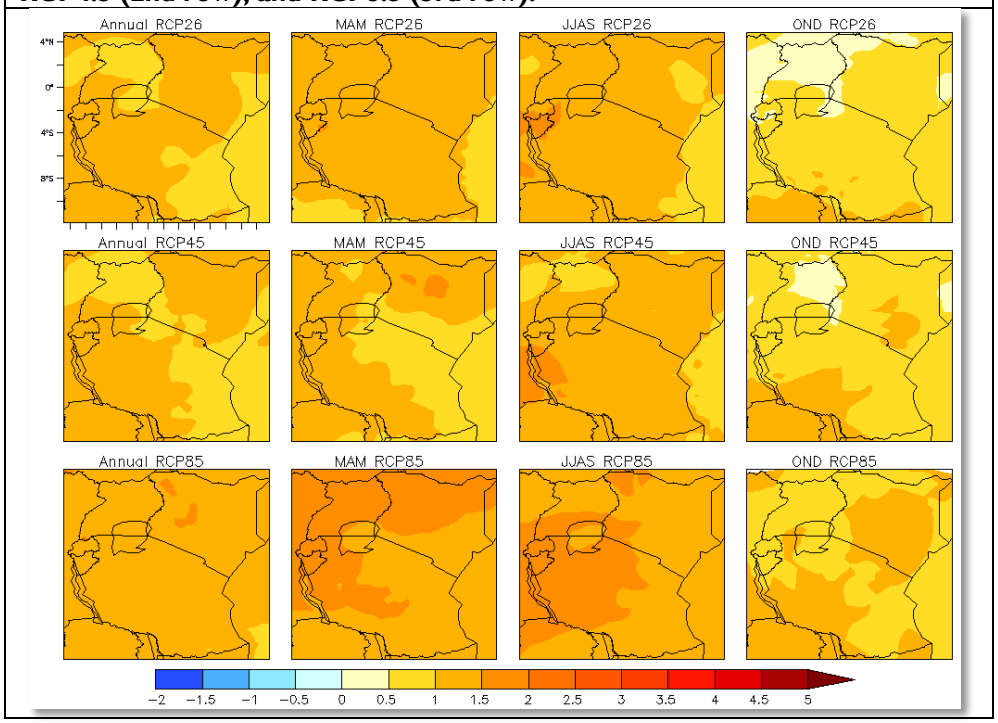

Figure 7: Projected maximum temperature changes over the EAC by the 2030s in annual (1st column), MAM (2nd column), JJAS (3rd column), OND (4th column). Each row corresponds to emission scenarios: RCP2.6 (1st row), RCP4.5 (2nd row), and RCP8.5 (3rd row).

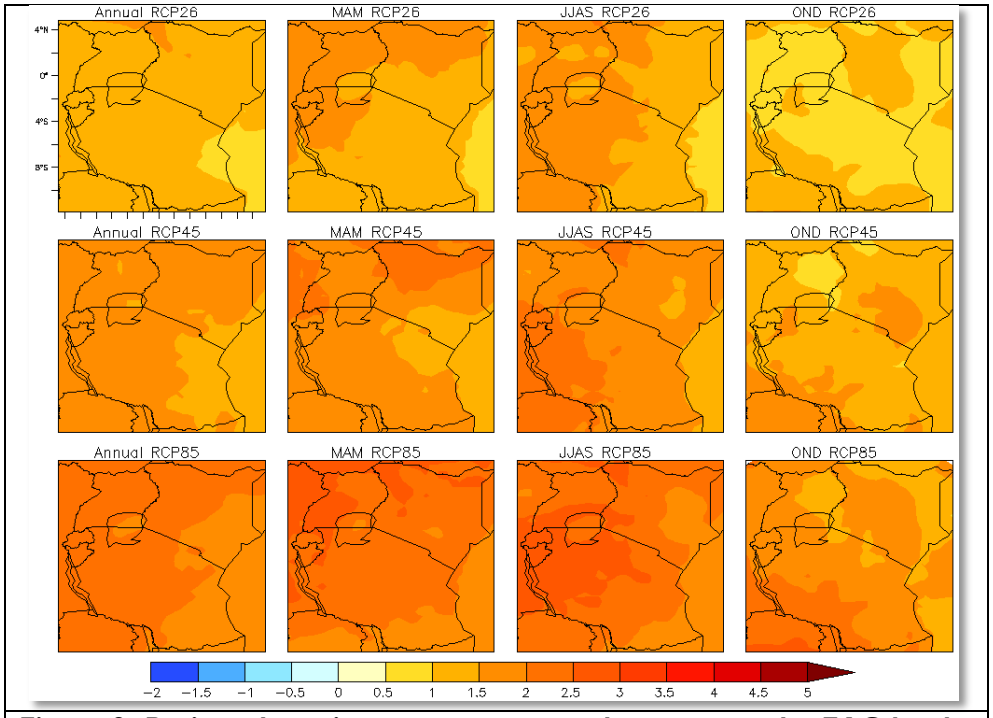

Figure 8: Projected maximum temperature changes over the EAC by the 2050s in annual (1st column), MAM (2nd column), JJAS (3rd column), OND (4th column). Each row corresponds to emission scenarios: RCP2.6 (1st row), RCP4.5 (2nd row), and RCP8.5 (3rd row).

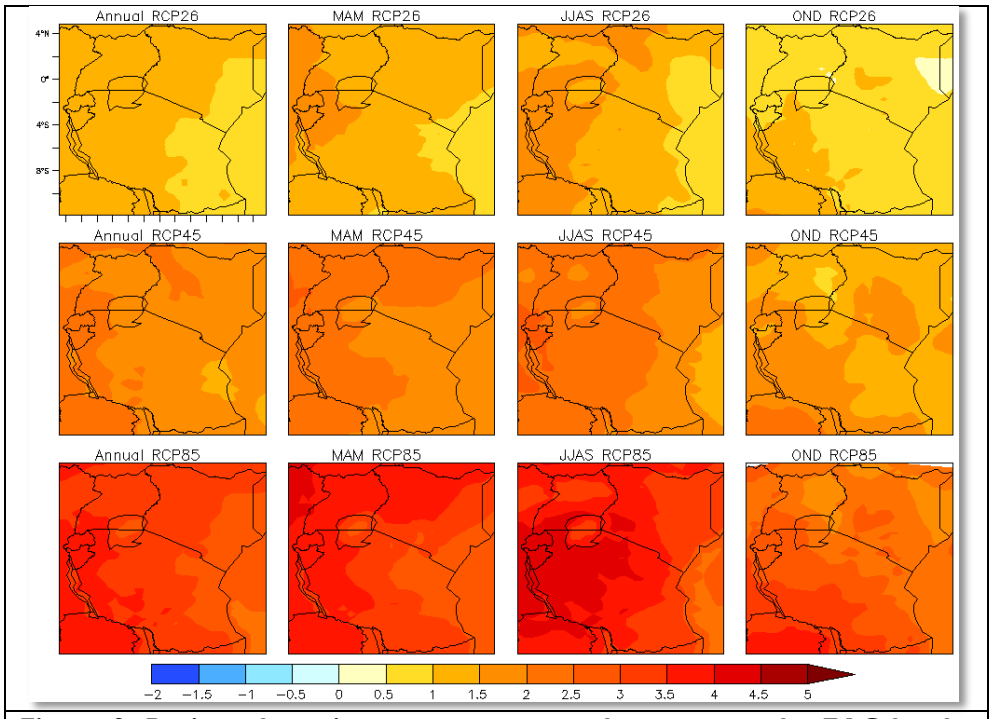

Figure 9: Projected maximum temperature changes over the EAC by the 2070s in annual (1st column), MAM (2nd column), JJAS (3rd column), OND (4th column). Each row corresponds to emission scenarios: RCP2.6 (1st row), RCP4.5 (2nd row), and RCP8.5 (3rd row).

MINIMUM TEMPERATURE

The projected changes in the minimum temperatures through time for the three scenarios are shown in Figures 10-13. The results suggest that there will likely be a greater increase in the minimum than the maximum temperatures in future. By 2020, annual minimum temperatures will likely be 0.5 to 1.5°C higher under the RCP2.6 and the RCP4.5 scenarios but 1.0 to 2.0°C higher under the RCP8.5 scenario over most parts of the EAC region. By 2030, almost all the EAC region will likely be 1.0 to 2.5°C warmer than the base period, with the greatest warming expected during the dry season months (JJAS) under the RCP8.5 scenario. By 2070, the projected increase in the annual minimum temperatures will likely be 4 to 5°C higher under the RCP8.5 scenario relative to the base period.

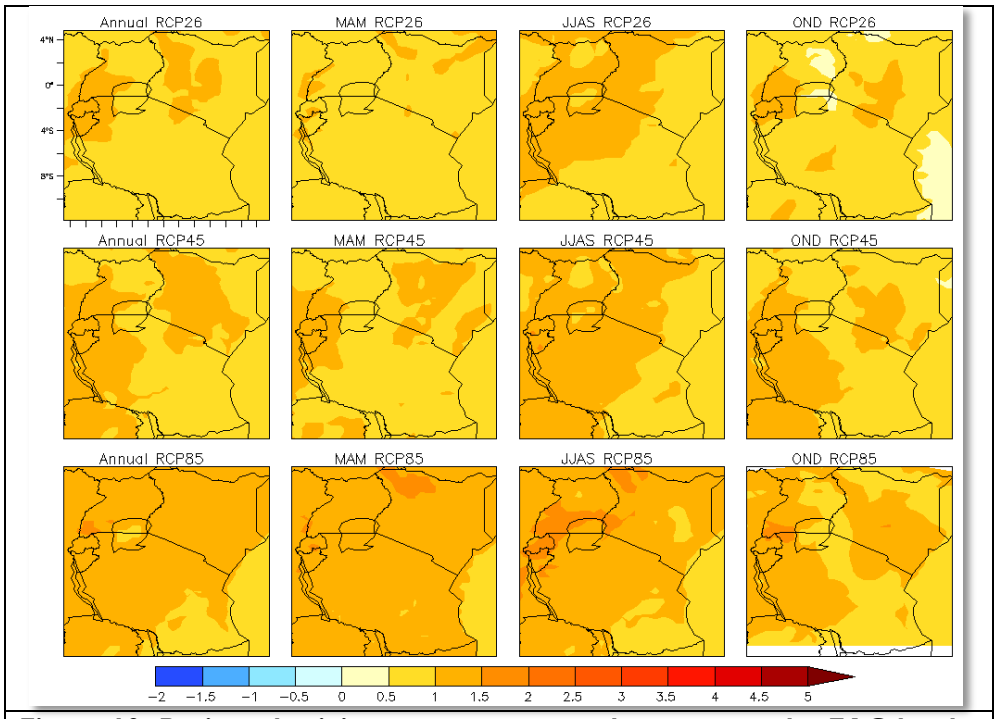

Figure 10: Projected minimum temperature changes over the EAC by the 2020s in annual (1st column), MAM (2nd column), JJAS (3rd column), OND (4th column). Each row corresponds to emission scenarios: RCP2.6 (1st row), RCP4.5 (2nd row), and RCP8.5 (3rd row).

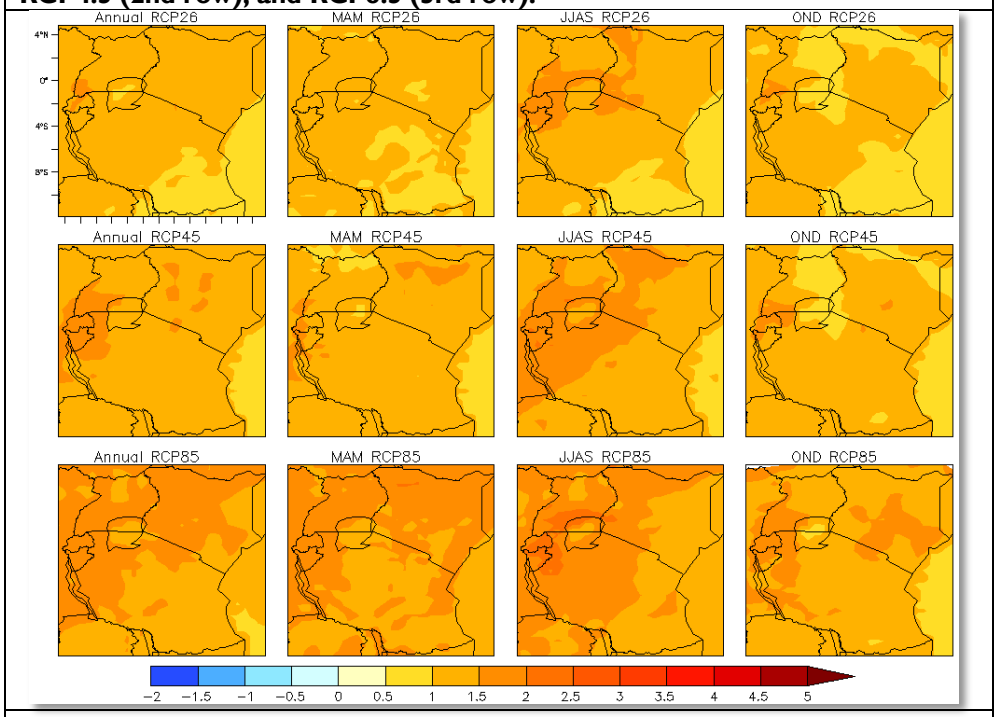

Figure 11: Projected minimum temperature changes over the EAC by the 2030s in annual (1st column), MAM (2nd column), JJAS (3rd column), OND (4th column). Each row corresponds to emission scenarios: RCP2.6 (1st row), RCP4.5 (2nd row), and RCP8.5 (3rd row).

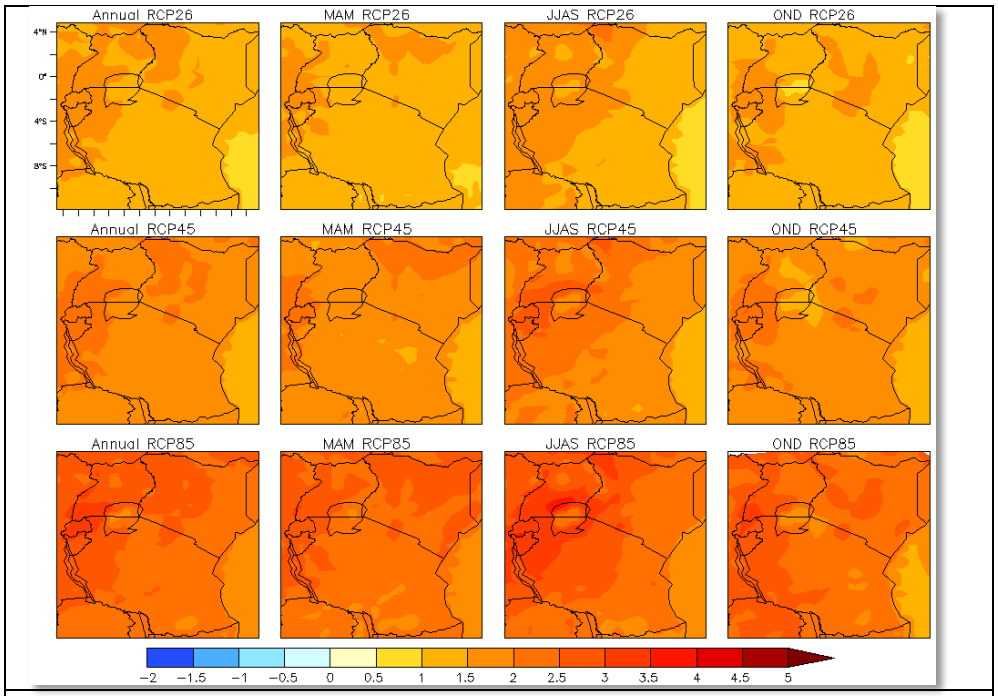

Figure 12: Projected minimum temperature changes over the EAC by the 2050s in annual (1st column), MAM (2nd column), JJAS (3rd column), OND (4th column). Each row corresponds to emission scenarios: RCP2.6 (1st row), RCP4.5 (2nd row), and RCP8.5 (3rd row).

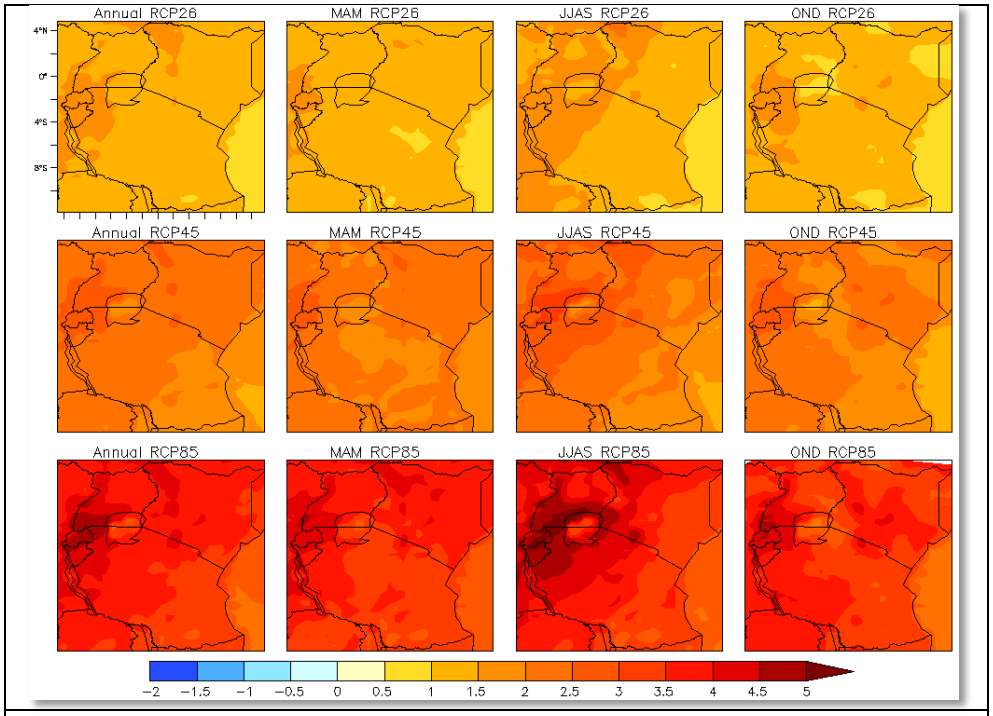

Figure 13: Projected minimum temperature changes over the EAC by the 2070s in annual (1st column), MAM (2nd column), JJAS (3rd column), OND (4th column). Each row corresponds to emission

scenarios: RCP2.6 (1st row), RCP4.5 (2nd row), and RCP8.5 (3rd row).

MAPPING OF EXTREME EVENTS—CHANGES IN THE PROJECTED RAINFALL AND TEMPERATURE EXTREMES

Climate-related extremes, such as floods and droughts, present significant challenges to nations worldwide, especially developing countries. The impacts of such events have undermined the gains made by developing countries and their global partners to meet their national development goals. The IPCC assessment in 2017 indicated that the severity and frequency of extreme events are increasing over parts of the world, with future projections showing continued increase at global, regional, and local scales (IPCC 2007, 2013). The expected changes in future climate extremes will likely force disaster managers to come up with new strategies for managing them since coping and response mechanisms and economic planning for disasters based on past vulnerabilities may no longer be adequate (Sperling and Szekely 2005).

Increase or decrease in extremes may result when the mean of a distribution changes (Figure 14), or when the variance changes, or when both the mean and variance change. The modifications of temperature and rainfall may result in changes in the intensity and frequency of these events.

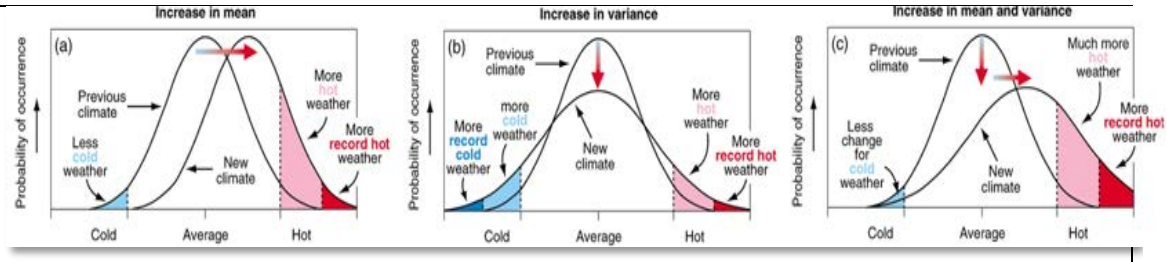

Figure 14: Normal distribution curve showing various hypothetical changes in extreme events. The figure shows changes in extreme temperature events due to (a) changes in mean, (b) changes in variance, and (c) changes in mean and variance (Source: IPCC 2013).

DATA AND METHODS

There are two approaches to generating the indices for extreme events. The first method uses percentile-based thresholds, the second uses fixed thresholds. These approaches are suitable for assessing moderate extremes, which usually occur a few times every year. Other high-impact, once-in-a-decade extreme events may be better assessed through other methods that model the occurrence of these events at the tail end of the distribution, e.g., Generalized Extreme Value and Generalized Pareto distributions (Coles 2001). Percentile-based thresholds were used in this assessment since they are better suited for areas with variable climate such as East Africa. Projected changes were quantified by calculating the differences between the future and the historical percentiles. The study focused on December–February (DJF), MAM, JJAS, and OND seasons using daily datasets. The base period was 1971–2000 and the analysis periods were 2006–2035, 2016–2045, 2036–2065 and 2056–2085.

DIFFERENCE IN THE 5TH PERCENTILE OF RAINFALL

Figures 15–18 show the difference between the future 5th percentile and the baseline 5th percentile for 2020, 2030, 2050, and 2070 periods during the DJF, MAM, JJAS, and OND seasons. During the DJF season, slight decrease (> -0.2mm) in the 5th percentile is expected in the southwestern parts of the Eastern Africa region while a slight increase (> +0.16mm) is expected in the southeastern parts of Tanzania. The spatial patterns of rainfall are similar for all the scenarios (Figure 5a). Similar patterns for the three scenarios are observed during MAM (Figure 5b). An increase in the 5th percentile was observed over the Indian Ocean and over a few areas in the coastal parts of Eastern Africa. Significant changes are observed under the low concentration pathway (RCP2.6) in the southwestern parts of the region. No significant changes are observed inland of the Eastern Africa region for all the scenarios. During the JJAS season, changes are observed over the southeastern parts of the domain (Figure 5c). Significant changes are observed over southern parts of the Eastern Africa region under RCP2.6 scenario during the OND season (Figure 5d). Several parts of the domain will likely experience increase in the 5th percentile during the 2050 and 2070 periods under the RCP4.5 and RCP8.5 scenarios.

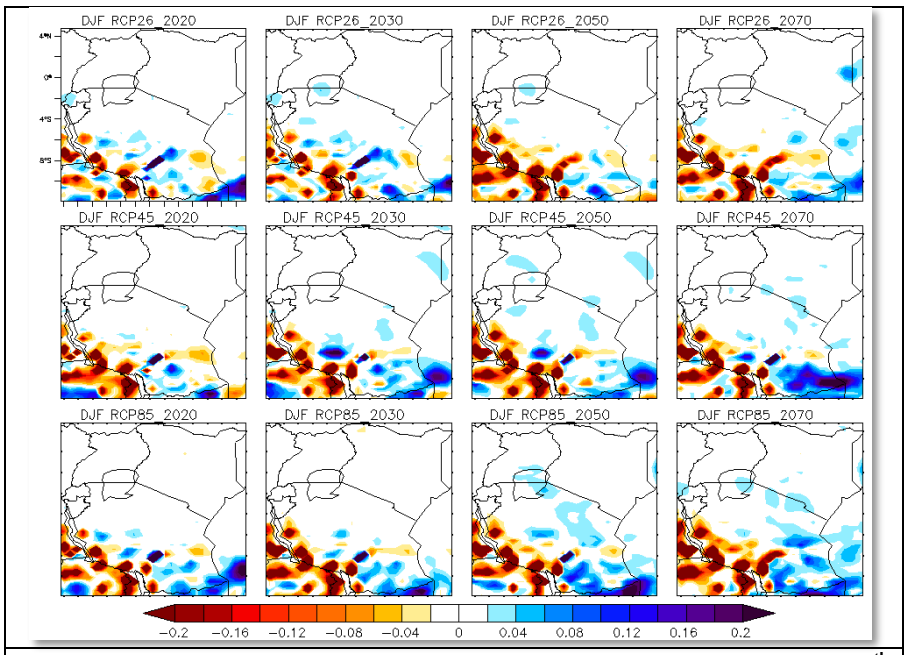

Figure 15: Differences between the future and baseline (1971–2000) 5th percentiles of rainfall in millimeters during the DJF season over the Eastern Africa region under the RCP2.6, RCP4.5, and RCP8.5 scenarios.

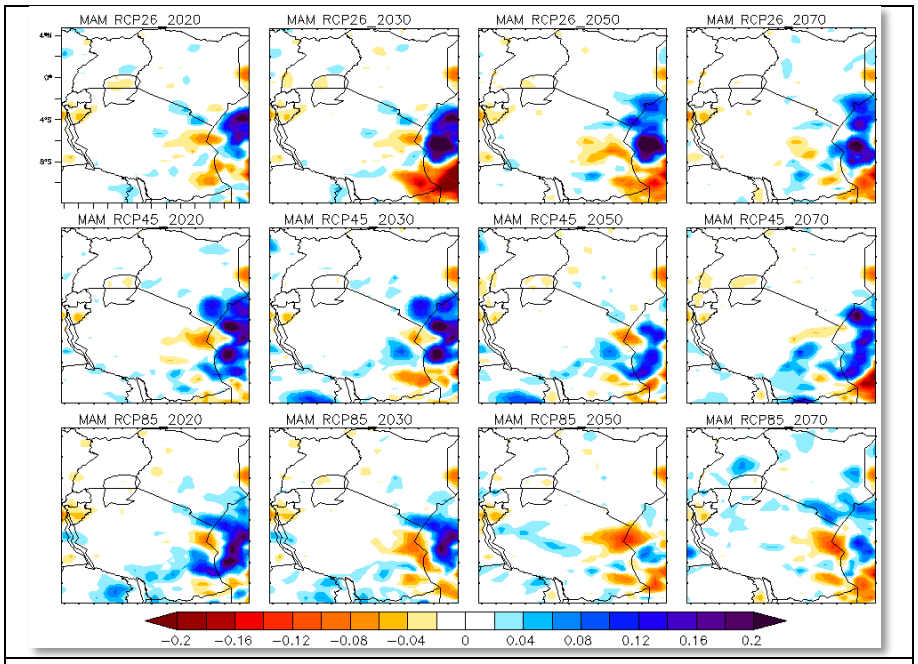

Figure 16: Differences between the future and baseline (1971–2000) 5th percentiles of rainfall in millimeters during the MAM season over the Eastern Africa region under the RCP2.6, RCP4.5, and RCP8.5 scenarios.

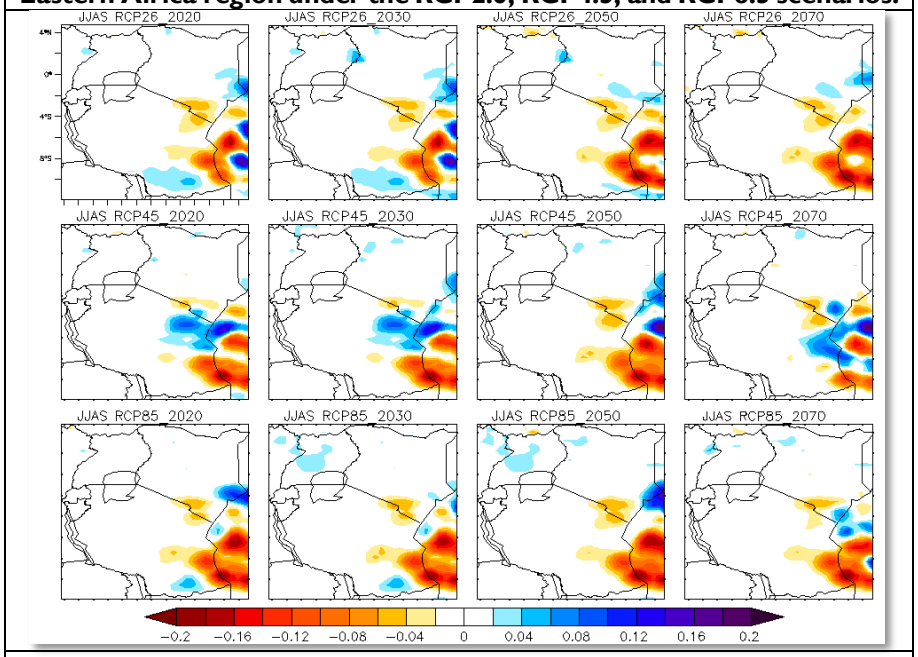

Figure 17: Differences between the future and baseline (1971–2000) 5th percentiles of rainfall in millimeters during the JJAS season over the Eastern Africa region under the RCP2.6, RCP4.5, and RCP8.5 scenarios.

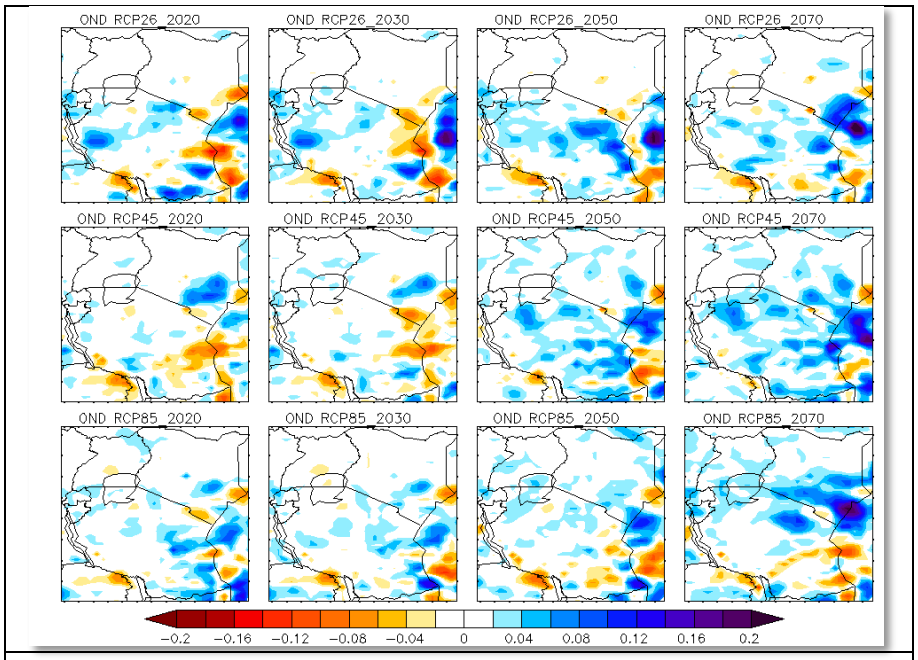

Figure 18: Differences between the future and baseline (1971–2000) 5th percentiles of rainfall in millimeters during the OND season over the Eastern Africa region under the RCP2.6, RCP4.5, and RCP8.5 scenarios.

DIFFERENCE IN THE 95TH PERCENTILE OF RAINFALL

The difference between the future 95th and the baseline 95th percentile in millimeters for rainfall was calculated and is shown in Figures 18–21. Increases of 1–6 millimeters are observed in the southern parts of the Eastern Africa region (Figure 6a). A few places over Kenya are expected to experience decreases of 1–4 millimeters with the northern parts of the domain experiencing no significant change. During the MAM season, the coastal parts of Kenya and Tanzania, Lake Victoria and northeastern parts of Kenya are expected to experience a decrease in rainfall (Figure 6b). Increases of 1–5 millimeters are expected over most of Tanzania and few parts of Kenya for the RCP4.5 and RCP8.5 scenarios. A decrease is expected over most parts of the domain during JJAS with increase in the 95th percentile expected over Uganda and western parts of Kenya (Figure 6c). During the OND season, most parts are expected to experience increase in the 95th percentile; only the southern parts of Tanzania are expected to experience a decrease (Figure 6d).

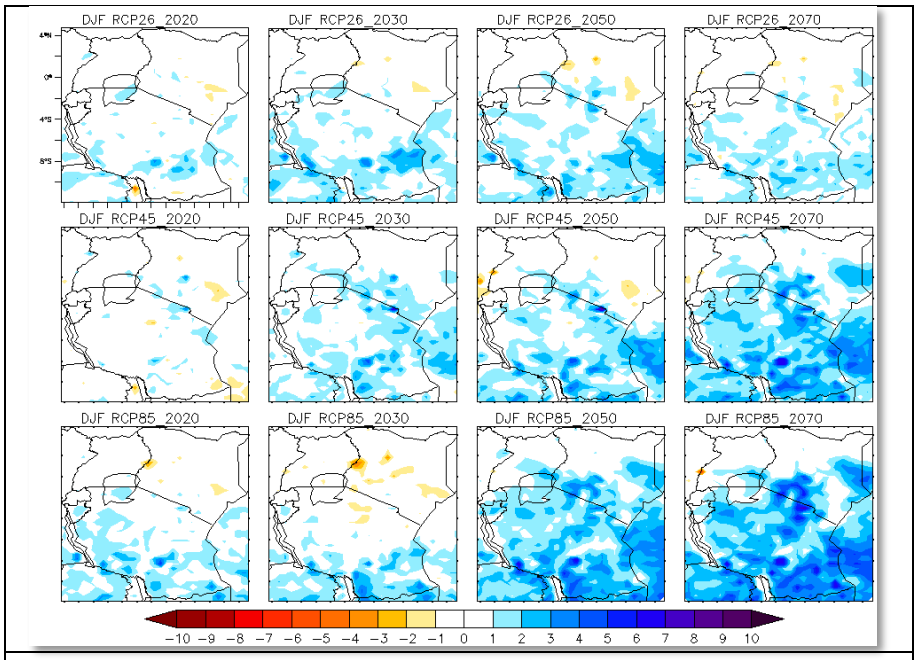

Figure 19: Differences between the future and baseline (1971–2000) 95th percentiles of rainfall in millimeters during the DJF season over the Eastern Africa region under the RCP2.6, RCP4.5, and RCP8.5 scenarios.

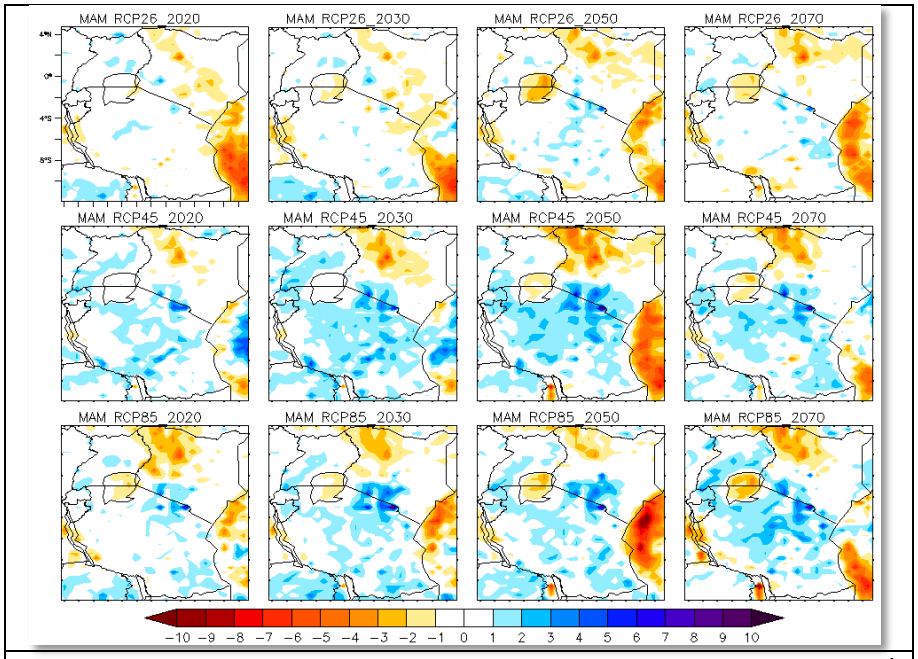

Figure 20: Differences between the future and baseline (1971–2000) 95th percentiles of rainfall in millimeters during the MAM season over the Eastern Africa region under the RCP2.6, RCP4.5, and RCP8.5 scenarios.

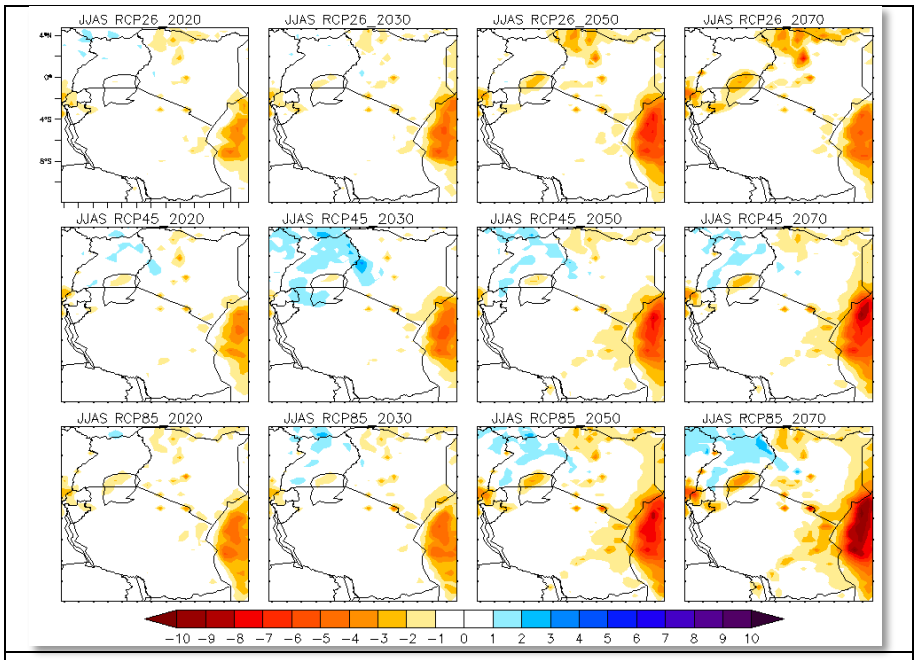

Figure 21: Differences between the future and baseline (1971–2000) 95th percentiles of rainfall in millimeters during the JJAS season over the Eastern Africa region under the RCP2.6, RCP4.5, and RCP8.5 scenarios.

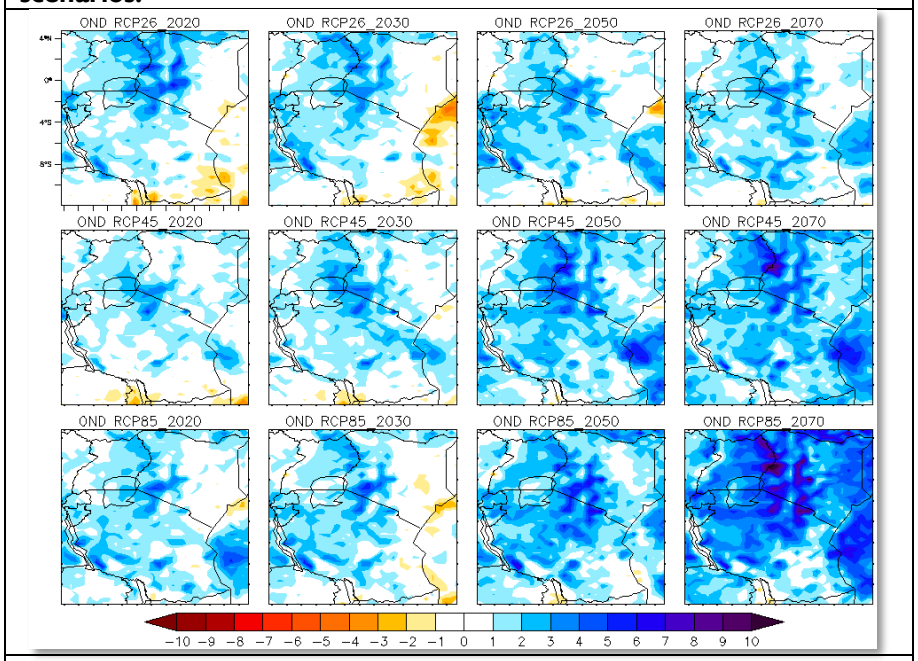

Figure 22: Differences between the future and baseline (1971–2000) 95th percentiles of rainfall in millimeters per day for the OND season over the Eastern Africa region under the RCP2.6, RCP4.5, and RCP8.5 scenarios.

DIFFERENCE IN THE 10TH PERCENTILE OF THE MAXIMUM TEMPERATURE

The 10th percentile was calculated for the maximum and minimum temperature under the three RCPs for the periods, 2020, 2030, 2050, and 2070 as shown in Figures 7a–7d. During the DJF season (Figure 23) marked warming is expected over most parts of the Eastern Africa region, with RCP8.5 being the warmest in the far future (2070). For the MAM season, the 2050 and 2070 periods are expected to record an increase in the 95th percentile over the northern parts of Eastern Africa (Figure 24). The highest increase is expected during the 2070 period under RCP8.5 scenario. Increase in the 10th percentile starts from the western parts during the JJAS season with the highest increases expected in the northwestern parts of the Eastern Africa region (Figure 25). An increase of between 1.5˚C and 2.5˚C is expected in the eastern parts of the Eastern Africa region during OND (Figure 26).

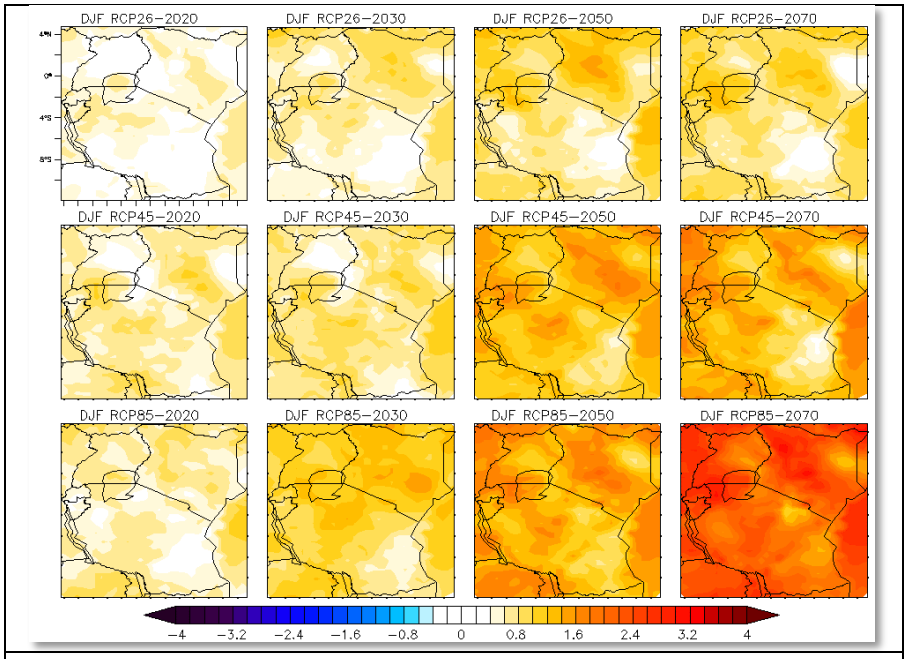

Figure 23: Differences between the future and baseline (1971–2000) 10th percentiles of the maximum temperature in degrees Celsius for the DJF season over the Eastern Africa region under the RCP2.6, RCP4.5, and RCP8.5 scenarios.

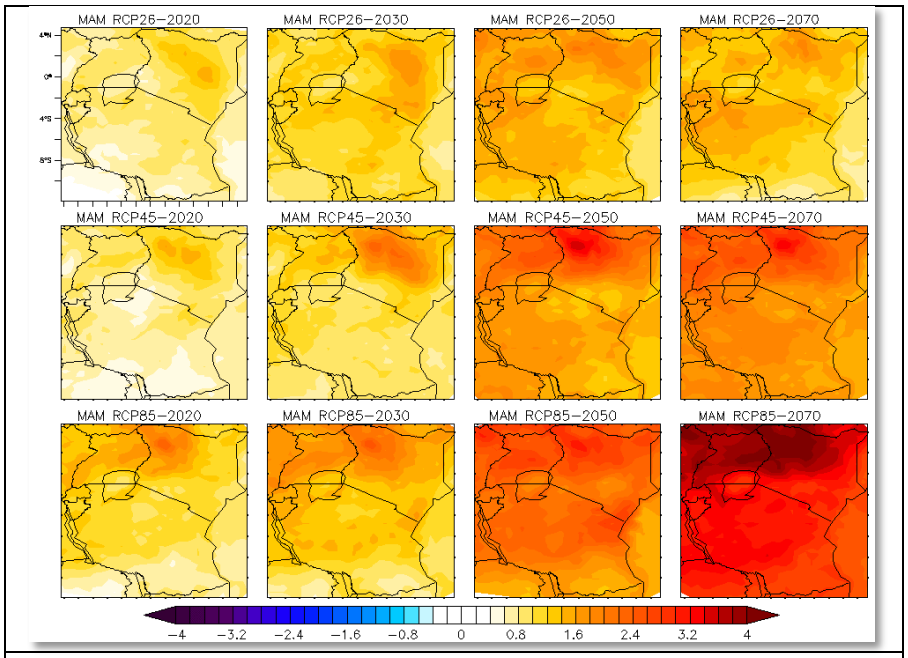

Figure 24: Differences between the future and baseline (1971–2000) 10th percentiles of the maximum temperature in degrees Celsius for the MAM season over the Eastern Africa region under the RCP2.6, RCP4.5, and RCP8.5 scenarios.

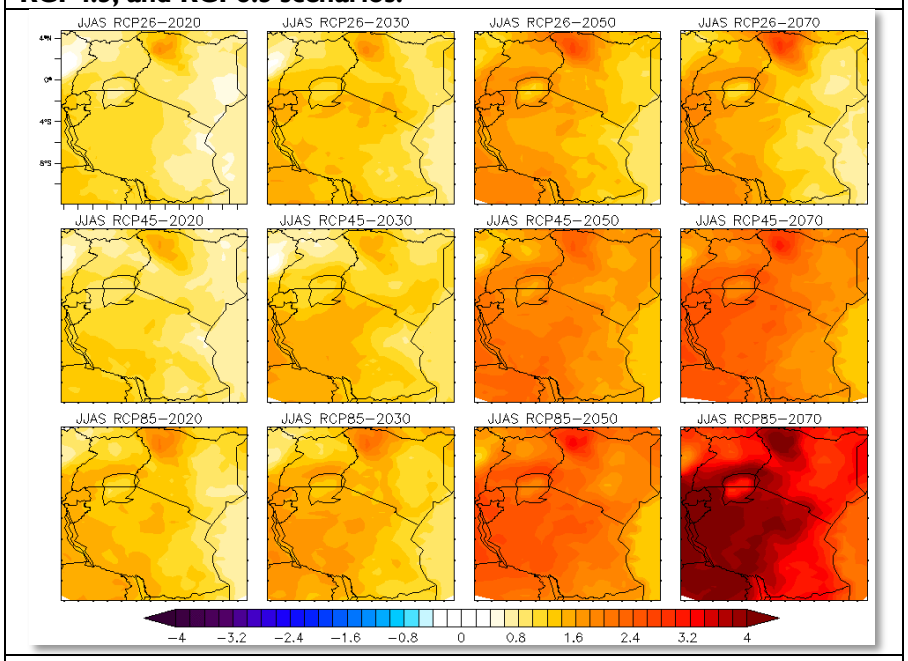

Figure 25: Differences between the future and baseline (1971–2000) 10th percentiles of the maximum temperature in degrees Celsius for the JJAS season over the Eastern Africa region under the RCP2.6, RCP4.5, and RCP8.5 scenarios.

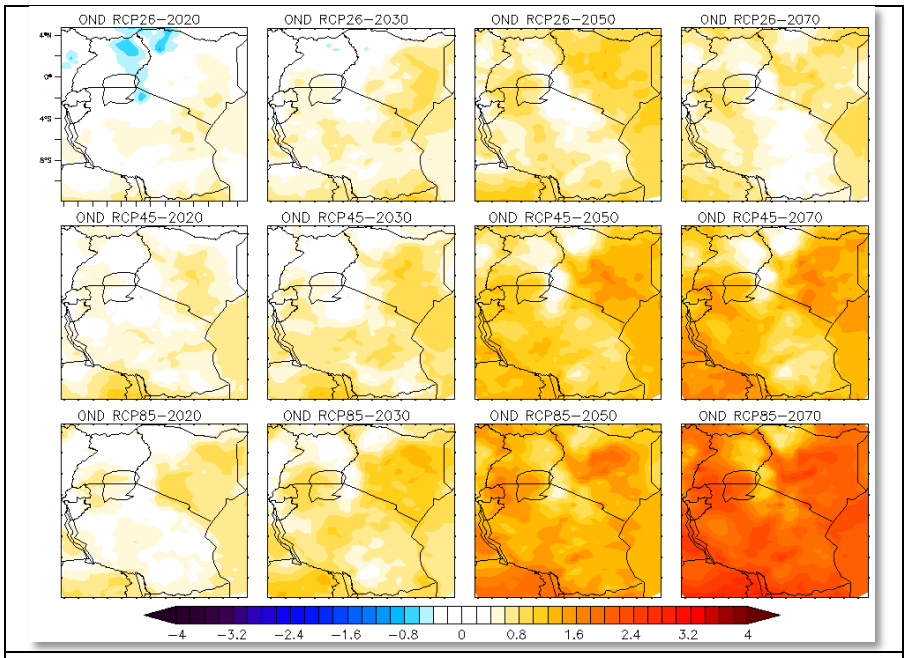

Figure 26: Differences between the future and baseline (1971–2000) 10th percentiles of the maximum temperature in degrees Celsius for the OND season over the Eastern Africa region under the RCP2.6, RCP4.5, and RCP8.5 scenarios.

DIFFERENCE IN THE 90TH PERCENTILE OF MAXIMUM TEMPERATURE

Decrease in the 90th percentile of maximum temperature is expected over the central parts of Tanzania (Figure 26). Increase in the 90th percentile of maximum temperature of 1.6˚C and above are expected to start by 2030 under the RCP8.5 scenario. During MAM, increases are expected to in the region in general (Figure 27). Areas around Lake Victoria are expected to experience increase during the JJAS season (Figure 28). Areas around Nairobi are also expected to experience some of the highest increases, which could be attributed to urbanization. During OND, increases will be expected to increase from south western parts of the region and along the Rift Valley in Kenya (Figure 29).

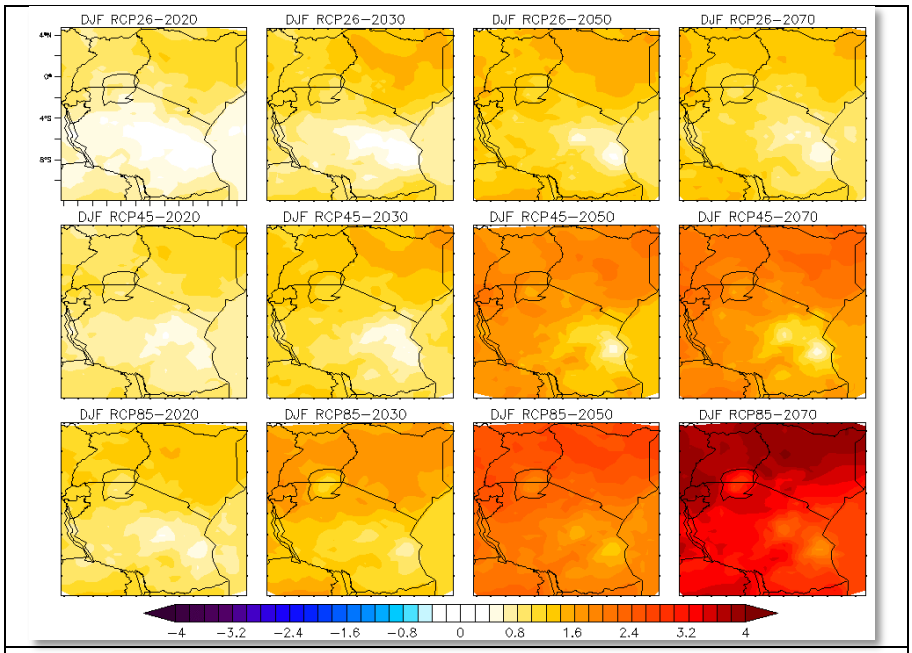

Figure 27: Differences between the future and baseline (1971–2000) 90th percentiles of the maximum temperature in degrees Celsius for the DJF season over the Eastern Africa region under the RCP2.6, RCP4.5, and RCP8.5 scenarios.

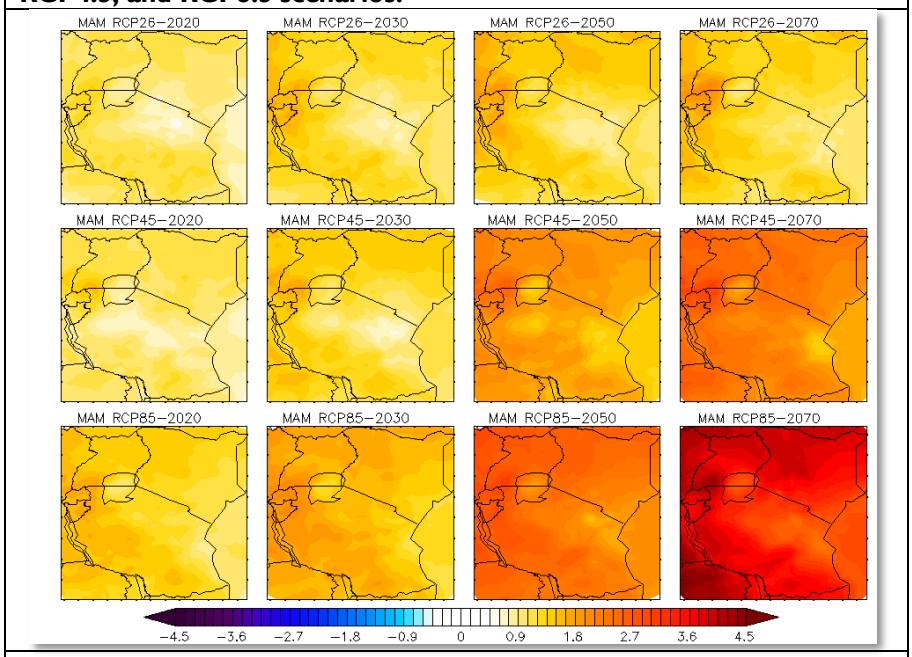

Figure 28: Differences between the future and baseline (1971–2000) 90th percentiles of the maximum temperature in degrees Celsius for the MAM season over the Eastern Africa region under the RCP2.6, RCP4.5, and RCP8.5 scenarios.

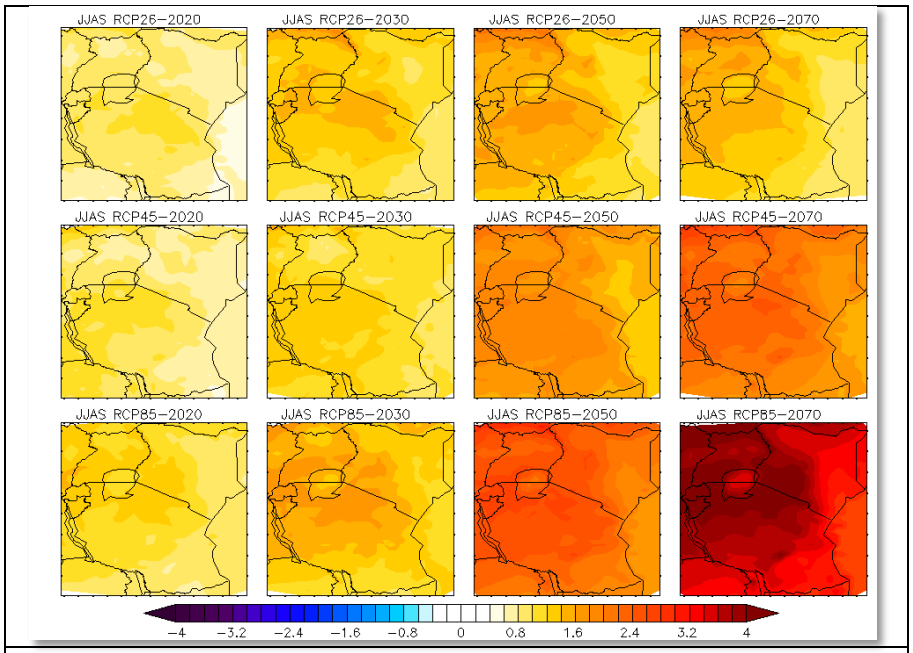

Figure 29: Differences between the future and baseline (1971–2000) 90th percentiles of the maximum temperature in degrees Celsius for the JJAS season over the Eastern Africa region under the RCP2.6, RCP4.5, and RCP8.5 scenarios.

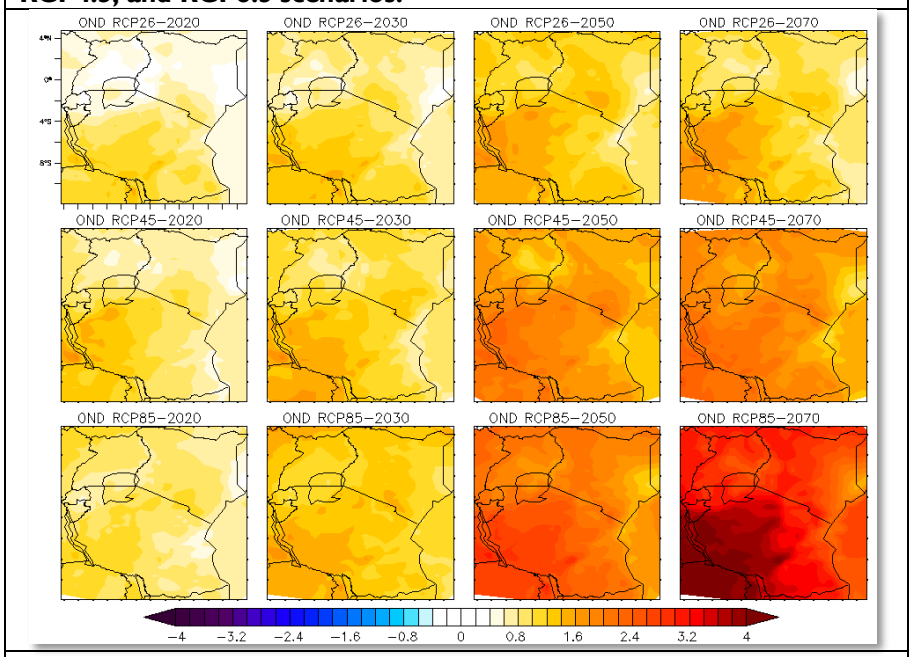

Figure 30: Differences between the future and baseline (1971–2000) 90th percentiles of the maximum temperature in degrees Celsius for the OND season over the Eastern Africa region under the RCP2.6, RCP4.5, and RCP8.5 scenarios.

DIFFERENCE IN THE 10TH PERCENTILE OF THE MINIMUM TEMPERATURE

Increases in the 10th percentile of the minimum temperature are expected in most parts of the region except the LVB in Tanzania, Kenya, and Uganda during the DJF season (Figure 31). Most of the region is expected to experience an increase greater than one degree Celsius during the MAM, JJAS, and OND seasons with the minimum temperature recording some of the highest increase under the RCP8.5 scenario (Figures 32, 33, and 34).

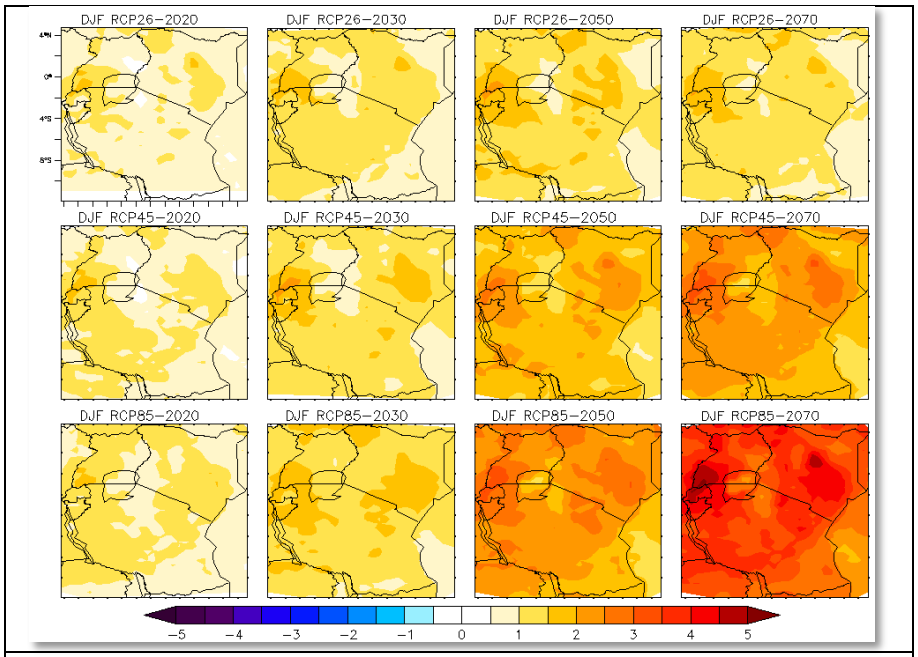

Figure 31: Differences between the future and baseline (1971–2000) 10th percentiles of the minimum temperature in degrees Celsius for the DJF season over the Eastern Africa region under the RCP2.6, RCP4.5, and RCP8.5 scenarios.

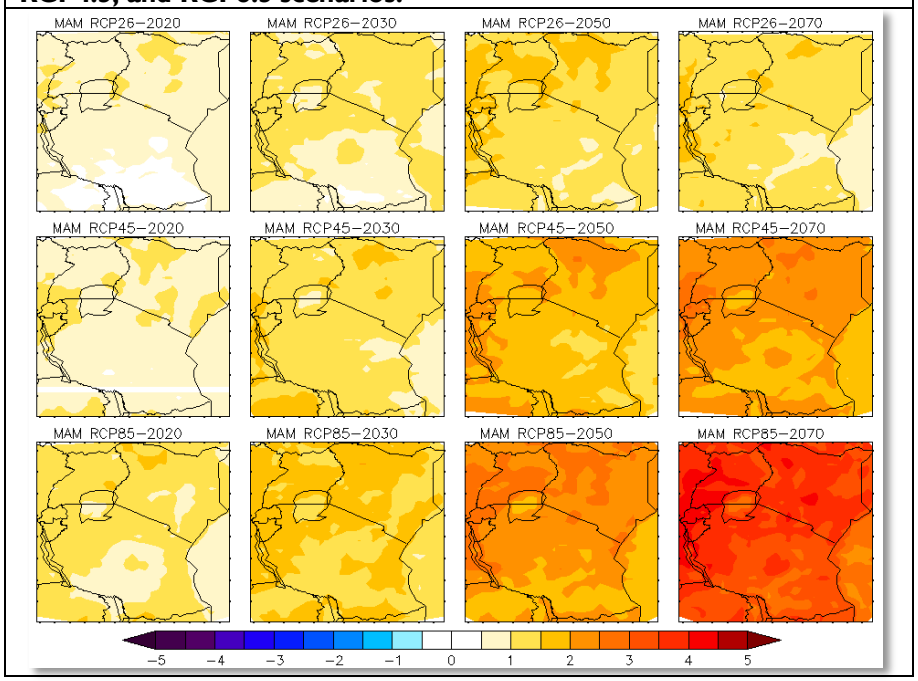

Figure 32: Differences between the future and baseline (1971–2000) 10th percentiles of the minimum temperature in degrees Celsius for the MAM season over the Eastern Africa region under the RCP2.6, RCP4.5, and RCP8.5 scenarios.

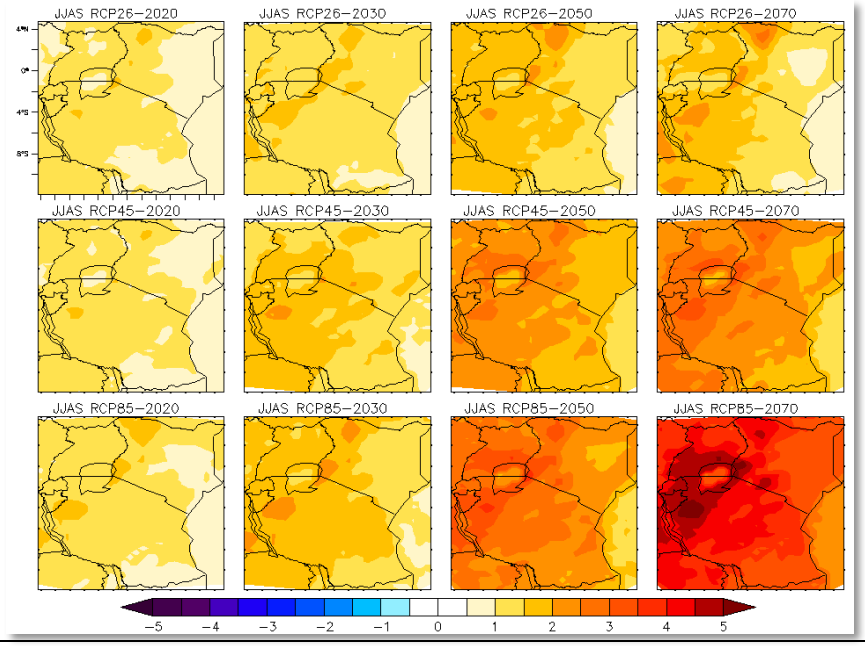

Figure 33: Differences between the future and baseline (1971–2000) 10th percentiles of the minimum temperature in degrees Celsius for the JJAS season over the Eastern Africa region under the RCP2.6, RCP4.5, and RCP8.5 scenarios.

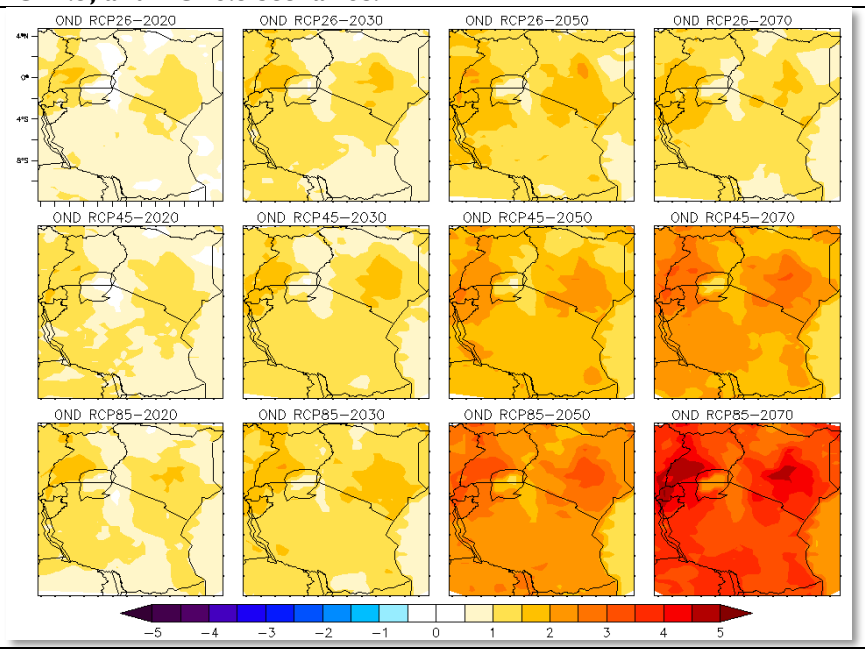

Figure 34: Differences between the future and baseline (1971–2000) 10th percentiles of the minimum temperature in degree Celsius for the OND season over the Eastern Africa region under the RCP2.6, RCP4.5, and RCP8.5 scenarios.

DIFFERENCE IN THE 90TH PERCENTILE OF THE MINIMUM TEMPERATURE

During the DJF season, an increase of more than 1°C in the 90th percentile of the minimum temperature is expected over northern Kenya and southwestern Uganda (Figure 35). All over the region, increases are expected during the MAM season (Figure 36). The same is expected for both the JJAS and the OND seasons (Figures 37 and 38).

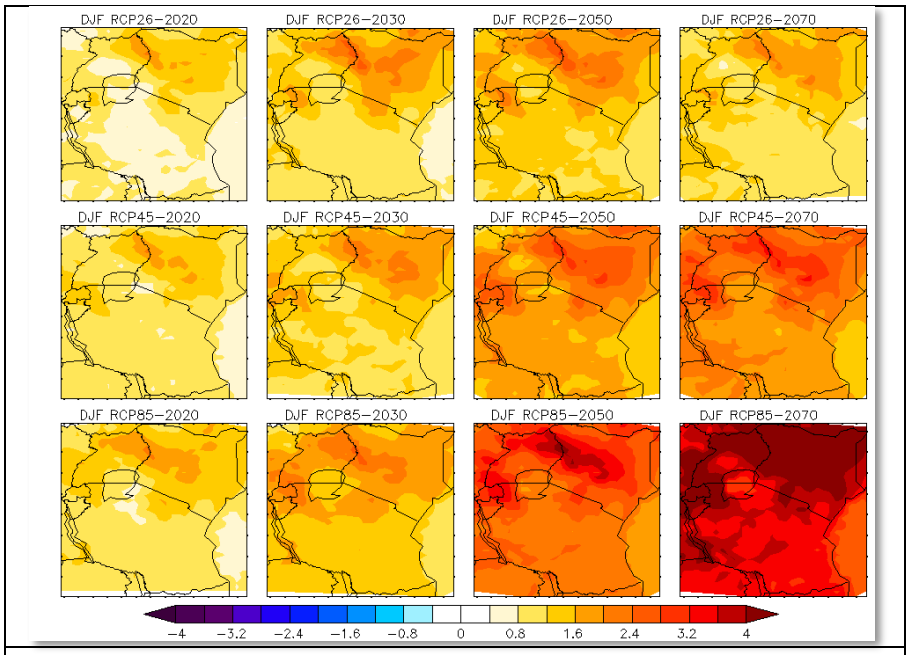

Figure 35: Differences between the future and baseline (1971–2000) 10th percentiles of the minimum temperature in degrees Celsius for the DJF season over the Eastern Africa region under the RCP2.6, RCP4.5, and RCP8.5 scenarios.

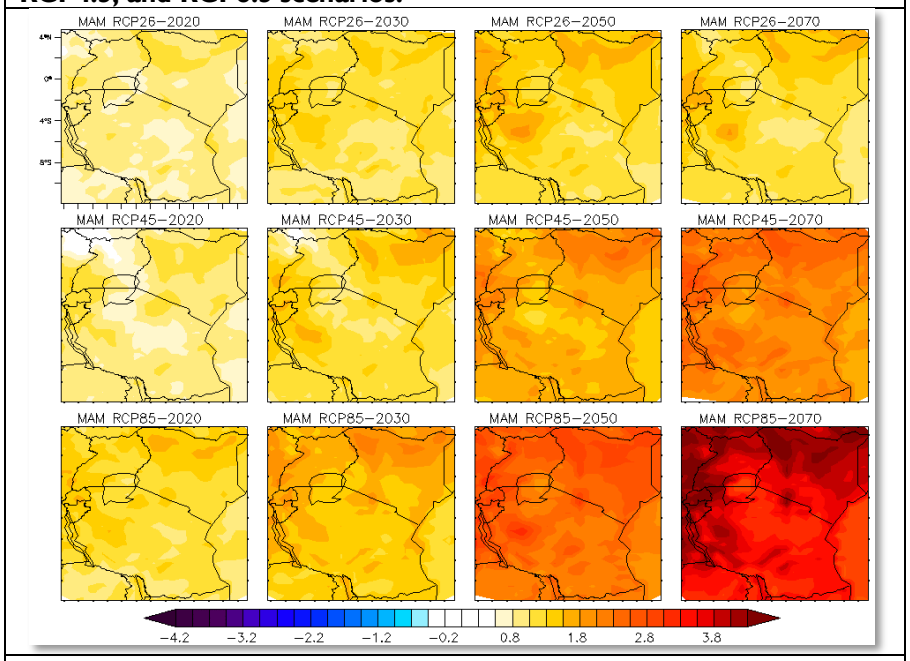

Figure 36: Differences between the future and baseline (1971–2000) 10th percentiles of the minimum temperature in degrees Celsius for

the MAM season over the Eastern Africa region under the RCP2.6, RCP4.5, and RCP8.5 scenarios.

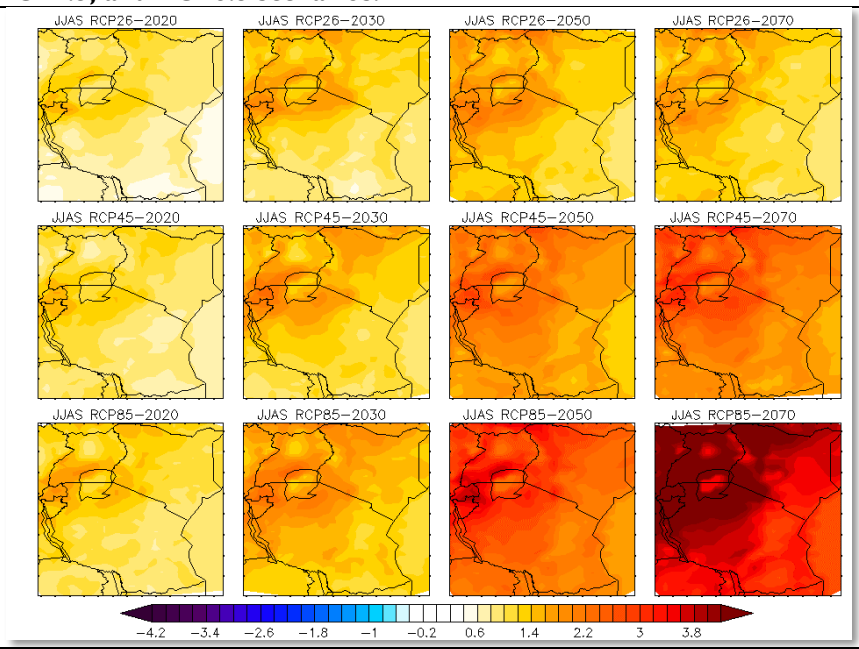

Figure 37: Differences between the future and baseline (1971–2000) 10th percentiles of the minimum temperature in degrees Celsius for the JJAS season over the Eastern Africa region under the RCP2.6, RCP4.5, and RCP8.5 scenarios.

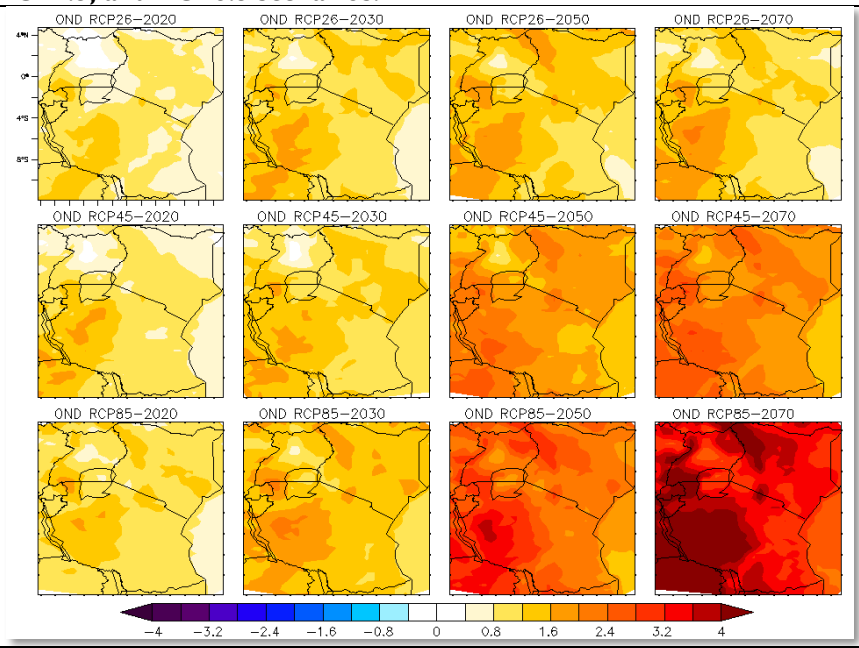

Figure 38: Differences between the future and baseline (1971–2000) 10th percentiles of the minimum temperature in degrees Celsius for the OND season over the Eastern Africa region under the RCP2.6, RCP4.5, and RCP8.5 scenarios.

HIGHLIGHTS

MODELING

- The study focused on DJF, MAM, JJAS, and OND seasons using daily datasets. The base period was 1971–2000 while the analysis periods were 2006–2035 (2020s), 2016–2045 (2030s), 2036–2065 (2050s), and 2056–2085 (2070s).
- The historical climate baseline was 1950–2005 and the period 1971–2000 was used as a reference for the present climate.
- The projected climate changes for each time window were calculated as the difference between the future time windows (averages calculated over 30 years) and the reference period. For example, the rainfall change by the 2070s was computed based on the difference in average rainfall between 2055–2085 and the reference period 1971–2000.
- The high-resolution regional climate projections were generated by the CORDEX program, initiated by the World Climate Research Program, to assess the future impacts of climate change at regional scales.
- The report used simulated data from the Rossby Center regional atmospheric model (RCA4) driven by the Earth system version of the Max Planck Institute for Meteorology (MPI-ESM-LR) coupled global climate model from the ongoing CORDEX program.
- The model was integrated into the CORDEX-Africa domain with a horizontal grid spacing of 0.44 degrees.
- Historical simulations were forced by observed natural and anthropogenic atmospheric composition covering the period 1950–2005; the projections for 2006–2100 were forced by Representative Concentration Pathways: RCP2.6, 4.5, and 8.5 as defined by the IPCC.
- The choice of the RCA model driven by the MPI-ESM-LR was based primarily on the availability of the model outputs for the three scenarios (RCP2.6, RCP4.5, and RCP8.5), as the other model runs were available for only one or two of the three scenarios. Downscaled data are available for historical (1951–2005) and projection (2006–2100) periods for the RCP2.6, RCP4.5, and RCP8.5 scenarios.
- The RCA model driven by MPI-ESM-LR better reproduces large-scale signals such as the ENSO and the IOD in the historical period over the Eastern Africa region than the RCA model driven by the other GCMs.
- The RCP2.6 low-level concentration pathway represents a peak in radiative forcing at ~3 W/m^2 (~490 ppm CO_2) by the mid-twenty-first century and then a decline to 2.6 W/m^2 by 2100. This scenario assumes optimistic mitigation measures and that the increase in the global average temperature will be kept below 2°C.
- RCP4.5 is a medium-level concentration pathway that is assumed to stabilize radiative forcing at 4.5 W/m^2 (~650 ppm CO_2) and that this value will not be exceeded by the year 2100.
- The RCP8.5 pathway represents a high-concentration pathway in which radiative forcing is assumed to reach 8.5 W/m^2 by the year 2100 (~1370 ppm CO_2) and then continues to rise thereafter. The RCP8.5 socioeconomic pathway is characterized by rapidly rising population and relatively slow income growth with modest rates of technological change and energy intensity improvements, leading in the long term, to high energy demands and greenhouse gas emissions in the absence of climate change policies.
- The data are at a resolution of 50 kilometers by 50 kilometers and cover the Africa domain.
- Increase or decrease in extremes may result when the mean of a distribution changes, when the variance changes, or when both the mean and variance change. The

modifications of temperature and rainfall may result in changes in the intensity and frequency of these events.

RESULTS

RAINFALL

- The projected changes in annual rainfall under the three different scenarios and time windows show relatively little change compared to the projected changes in seasonal rainfall. MAM rainfall decreases in northern part of East Africa and increases in southeastern areas.
- The long rains (MAM period) are projected to decrease over the northern part but increase over the southeastern part of the region.
- Projected annual rainfall shows a tendency to increase over the LVB except for JJAS in 2020 for RCP8.5 and 2070 for RCP2.6.

Attribute	2006–2035 (2020s)	2016–2045(2030s)	2036–2065(2050s)	2056–2085(2070s)
Short rain (OND)	Increase 5–25%	Increase 5–25%	Increase 25–50%	Increase 25–50%
JJAS rain (western and coastal rains)	Increase 25–50%	Increase 25–50%	Increase 50–75%	Increase 50–75%

MAXIMUM TEMPERATURE

- Projected temperature changes for the three different scenarios and time windows show relatively large changes compared to the projected changes in the seasonal components.
- By 2030, maximum temperatures during the long rains (MAM), the dry season (JJAS), and throughout the year will likely increase by 1.0–2.0°C over most parts of the region, but with spatial variation similar to that of 2020.
- The greatest potential warming will likely occur in the dry season (JJAS) and during the long rains (MAM) and least during the short rains (OND).
- In the far future (2070), projected annual maximum temperatures will likely be 0.5–1.5°C higher under RCP2.6, which is notably smaller than the changes anticipated by 2050. This is due to the reduction in radiative forcing expected toward the end of the century due to mitigation measures under the RCP2.6 scenario.
- In contrast, under the RCP8.5 scenario, the expected annual warming will likely result in temperatures 3.5–4.5°C higher than the reference period, with far greater warming expected during the dry season (JJAS).

Attribute	RCP 2.6	RCP 4.5	RCP 8.5
Increase in Maximum Temperature by 2030	0.5–1.0 degrees	0.5–1.0 degrees	0.5–1.5 degrees
Increase in Maximum Temperature by 2050	1.0–2.0 degrees	1.5–2.5 degrees	2.5–3.5 degrees
Increase in Maximum Temperature by 2070	0.5–1.5 degrees		3.5–4.5 degrees

MINIMUM TEMPERATURE

- The results suggest that there will likely be a greater increase in the minimum than the maximum temperatures in future.

- By 2030, almost all the EAC region will likely be 1.0–2.5°C warmer than the base period, with the greatest warming expected during the dry season months (JJAS) under the RCP8.5 scenario.
- By 2070, the projected increase in annual minimum temperatures will likely be 4–5°C higher under the RCP8.5 scenario relative to the base period.

Attribute	RCP 2.6	RCP 4.5	RCP 8.5
Increase in Minimum Temperature by 2020	0.5–1.5 degrees	0.5–1.5 degrees	1.0–2.0 degrees
Increase in Minimum Temperature by 2070			4.0–5.0 degrees

REFERENCES

Anyamba, A., K.J. Linthicum, J.L. Small, K.M. Collins, C.J. Tucker, E.W. Pak, S.C. Britch, J.R. Eastman, J.E. Pinzon, K.L. Russell, 2012: "Climate Teleconnections and Recent Patterns of Human and Animal Disease Outbreaks." *PLoS Neglected Trop. Dis.,*6, e1465.

Bhola, N., J.O. Ogutu, M.Y. Said, H.P. Piepho, H. Olff, 2012a: "The distribution of large herbivore hotspots in relation to environmental and anthropogenic correlates in the Mara Region of Kenya." *Journal of Animal Ecology.* 1268–1287.

Bhola, N., J.O. Ogutu, M.Y. Said, R.S. Reid, H.P. Piepho, H. Olff, 2012b: "Comparative changes in density and demography of large herbivores in Masai Mara Reserve and the adjacent Koyiaki Pastoral Ranch, Kenya." *Biodiversity and Conservation.* 1509–1530.

Birkett, C., R. Murtgudde, T. Allan, 1999: "Indian Ocean climate event brings floods to East Africa's lake and the Sudd marsh." *Geophysical Research Letters* 26: 1031–1034.

Burgiel, S.W., A.A. Muir: 2010. Invasive Species, Climate Change and Ecosystem-Based Adaptation: Addressing Multiple Drivers of Global Change. Global Invasive Species Programme (GISP), Washington, DC, and Nairobi, Kenya.

CAMCO, 2016a: Baseline report on climate change, Nairobi, Kenya.

CAMCO, 2016b: Baseline report for health, sanitation and human settlements sector. Vulnerability impacts and adaptation assessment in the Lake Victoria Basin. Nairobi, Kenya.

CAMCO, 2016c: Baseline report for terrestrial sector. Vulnerability impacts and adaptation assessment in the Lake Victoria Basin. Nairobi, Kenya.

Channel, R., M.V. Lomolino, 2000: "Dynamic biogeography and conservation of endangered species." *Nature* 403: 84–86.

Coles, S.G., 2001: *An Introduction to Statistical Modeling of Extreme Values.* Springer Series in Statistics, Springer, 224 pp.

Craig, M.H., I. Kleinschmidt, J.B. Nawn, D. Le Sueur, and B.L. Sharp, 2004: "Exploring 30 years of malaria case data in KwaZulu-Natal, South Africa: part I. The impact of climatic factors." *Tropical Medicine and International Health* 9: 1247–1257.

Endris, H.S., C. Lennard, B. Hewitson, A. Dosio, G. Nikulin, H.J. Panitz, 2015: "Teleconnection responses in multi-GCM driven CORDEX RCMs over Eastern Africa." *Climate Dynamics*, 1–26.

Endris, H.S., P. Omondi, S. Jain, C. Lennard, B. Hewitson, L. Chang'a, H.J. Panitz, 2013: "Assessment of the performance of CORDEX regional climate models in simulating East African rainfall." *Journal of Climate*, *26*(21), 8453–8475.

Fick, A.A., C.A. Myrick, L.J. Hansen, 2005: Potential impacts of global climate change on freshwater fisheries. A report for WWF, Gland, Switzerland.

Funk, C., G. Senay, A. Asfaw, J. Verdin, J. Rowland, J. Michaelson, G. Eilerts, D. Korecha, R. Choularton, 2005: Recent drought tendencies in Ethiopia and equatorial-subtropical eastern Africa. Washington DC, FEWS-NET.

Giorgi, F., 2006: "Climate change hot-spots." *Geophys. Res. Lett.,* 33, L08707, doi:10.1029/2006GL025734.

Giorgi, F., C. Jones, G.R. Asrar, 2009: "Addressing climate information needs at the regional level: the CORDEX framework." *World Meteorological Organization (WMO) Bulletin*, *58*(3), 175.

Githeko, A.K., W. Ndegwa, 2001: "Predicting malaria epidemics in the Kenyan Highlands using climate data: a tool for decision-makers." *Global Change and Human Health,* 2: 54–63.

ICPAC, 2016: Projected changes in rainfall and temperature over Greater Horn of Africa in different scenarios. In Support of: Planning for Resilience in East Africa through Policy, Adaptation, Research, and Economic Development (PREPARED) Project.

IPCC, 2001: *Climate Change 2001. Synthesis report.* Cambridge: Cambridge University Press.
IPCC, 2007a: *Climate Change 2007: Impacts, Adaptation and Vulnerability.* Cambridge: Cambridge University Press.
IPCC, 2007b: Climate Change 2007: *The Physical Science Basis. Contribution of Working Group I to the Fourth Assessment Report of the Intergovernmental Panel on Climate Change* [S. Solomon, D. Qin, M. Manning, Z. Chen, M. Marquis, K.B. Averyt, M. Tignor, H.L. Miller (eds.)]. Cambridge University Press, Cambridge, United Kingdom, and New York, NY.
IPCC, 2013: Climate Change 2013: *The Physical Science Basis. Contribution of Working Group I to the Fifth Assessment Report of the Intergovernmental Panel on Climate Change* [T.F. Stocker, D. Qin, G.-K. Plattner, M. Tignor, S.K. Allen, J. Boschung, A. Nauels, Y. Xia, V. Bex, P.M. Midgley (eds.)]. Cambridge University Press, Cambridge, United Kingdom, and New York, NY, 1535 pp.
IPCC, 2014: Climate Change 2014: Synthesis Report Contribution of Working Groups I, II and III to the Fifth Assessment Report of the Intergovernmental Panel on Climate Change [Core Writing Team, R.K. Pachauri, L.A. Meyer (eds.)]. IPCC, Geneva, Switzerland, 151 pp.
Kirilenko, A.P., A.M. Solomon, 1998: "Modeling dynamic vegetation response to rapid climate change using bioclimatic classification." *Climatic Change* 38: 15–49.
Lovett, J.C., G.F. Midgely, P.B. Barnard, 2005: "Climate change and ecology in Africa." *African Journal of Ecology* 43: 279–281.
Malcolm, J.R., A. Markham, R.P. Neilson, M. Garaci, 2002: "Estimated migration rates under scenarios of global climate change." *Journal of Biogeography* 29: 835–849.
Moss, R.H., J.A. Edmonds, K.A. Hibbard, M.R. Manning, S.K. Rose, D.P. Van Vuuren, T.J. Wilbanks, 2010: "The next generation of scenarios for climate change research and assessment." *Nature*, *463*(7282), 747–756.
Nikulin, G., C. Jones, F. Giorgi, G. Asrar, M. Büchner, R. Cerezo-Mota, E. van Meijgaard, 2012: "Precipitation climatology in an ensemble of CORDEX-Africa regional climate simulations." *Journal of Climate*, *25*(18), 6057–6078.
Ogutu, J.O., H.P. Piepho, H.T. Dublin, 2014: "Responses of phenology, synchrony and fecundity of breeding by African ungulates to interannual variation in rainfall." *Wildlife Research*. 698–717.
Ogutu, J.O., H.P. Piepho, H.T. Dublin, 2012: "Ostrich recruitment dynamics in relation to rainfall in the Mara-Serengeti ecosystem." Ostrich: *Journal of African Ornithology*. 119–136.
Ogutu, J.O., H.P. Piepho, M.Y. Said, S.C. Kifugo, 2014: "Herbivore dynamics and range contraction in Kajiado: Climate and land use changes, population pressures, governance, policy and human-wildlife conflicts." *Open Ecology Journal*. 9–31.
Ogutu, J.O., H.P. Piepho, H.T. Dublin, 2015: "Reproductive seasonality in African ungulates in relation to rainfall." *Wildlife Research*. 323–342.
Patz, J.A., D. Campbell-Lendrum, T. Holloway. J. A. Foley, 2005: "Impact of regional climate change on human health." *Nature* 438: 310–317.
PREPARED, 2013: Scoping Study on Vulnerability, Impacts and Adaptation Assessments (VIA).
PREPARED, 2014: Approach and Methodology for the Lake Victoria Basin Vulnerability, Impacts and Adaptation Assessment (VIA). Tetra Tech ARD.
Poole, J.H., 1989: "Announcing intent: the aggressive state of musth in African elephants." *Animal Behavior*. 37: 140–152.
Riahi, K., S. Rao, V. Krey, C. Cho, V. Chirkov, G. Fischer, P. Rafaj, 2011: "RCP 8.5-A scenario of comparatively high greenhouse gas emissions." *Climatic Change*, 109(1–2), 33–57.
Rich, K., F. Wanyioke, 2010: "An assessment of the regional and national socio-economic impacts of the 2007 Rift Valley fever outbreak in Kenya." *Am. J. Trop. Med. Hyg.,* 83 52–57.
Roessig, J.M., C.M. Woodley, J.J. Cech, Jr., and L.J. Hansen, 2004: "Effects of global climate change on marine and estuarine fishes and fisheries." *Reviews in Fish Biology and Fisheries* 14: 251–275.
Rubenstein, D.I., 1992: "The greenhouse effect and changes in animal behavior: effects on social

structure and life-history strategies" in *Global Warming and Biological Diversity*, R.L. Peters and T.E. Lovejoy, Eds., Yale University Press pp.180–192.

Simms, A., 2005: Africa: up in smoke? The second report from the Working Group on Climate Change and Development, New Economics Foundation, London.

Solomon, A.M., A.P. Kirilenko, 1997: "Climate change and terrestrial biomes: what if trees do not migrate?" *Global Ecology and Biogeography* 6: 139–148.

Sperling, F., F. Szekely, 2005: Disaster risk management in a changing climate. VARG, Washington DC.

Seitz, J., W. Nyangena, 2009: Economic Impact of Climate Change in the Eastern Africa Community (EAC), Toulouse, France and Eschborn, Germany: Global21 Consulting and Deutsche Gesellschaft für Technische Zusammenarbeit.

Sykes, M.T., I.C. Prentice, 1996: "Climate change, tree species distributions and forest dynamics: a case study in the mixed conifer/hardwoods zone of northern Europe." *Climatic Change* 34: 161–177.

Thirgood, S., A. Mosser, S. Tham, G. Hopcraft, E. Mwangomo, T. Mlengeya, M. Kilewo, J. Fryxell, A.R.E. Sinclair, M. Borner, 2004: "Can parks protect migratory ungulates? The case of the Serengeti wildebeest." *Animal Conservation* 7: 113–120.

Thompson, L.G., E. Mosley-Thompson, M.E. Davis, K.A. Henderson, H.H. Brecher, V.S. Zagorodnov, T.A. Mashiotta, P-N. Lin, V.N. Mikhalenko, D.R. Hardy, J. Beer, 2002: "Kilimanjaro ice core records: evidence of Holocene climate change in tropical Africa." *Science* 298: 589–593.

United Nations, Department of Economic and Social Affairs, Population Division, 2015: World Population Prospects: The 2015 Revision, Key Findings and Advance Tables. Working Paper No. ESA/P/WP.241.

Van Vuuren, D.P., J. Edmonds, M. Kainuma, K. Riahi, A. Thomson, K. Hibbard, T. Masui, 2011: "The representative concentration pathways: an overview." *Climatic change*, *109*, 5–31.

Vanacker, V., M. Linderman, F. Lupo, S. Flasse, E. Lambin, 2005: "Impact of short-term rainfall fluctuation on interannual land cover change in sub-Saharan Africa." *Global Ecology and Biogeography* 14: 123–135.

Wara, M.W., A.C. Ravelo, M.L. Delaney, 2005: "Permanent El Niño-like conditions during the Pliocene Warm Period." *Science* 309: 758–761.

Western, D., 2010a: "Conservation in an age of climate change." *Swara:* 1. 24–25.

Western, D., 2010b: "The Worst Drought: Tipping Point or Turning Point." *Swara:* 2.16–20.

World Bank, 2013: *Turn Down the Heat. The Climate Extremes, Regional Impacts, and the Case for Resilience.* Washington, DC: World Bank.

Zhou, G., N. Minakawa, A.K. Githeko, G. Yan, 2004: Association between climate variability and malaria epidemics in the East African highlands. Proceedings of the National Academy of Sciences of the United States of America. 101: 2375–2380.

U.S. Agency for International Development
PO Box 629
Village Market 00621
Nairobi, Kenya
Telephone +254 20 862 2000
Fax +254 20 862 2680/ 2682
http://www.usaid.gov/east-africa-regional